HYDROLOGICAL PROCESSES
Hydrol. Process. (2013)
Published online in Wiley Online Library
(wileyonlinelibrary.com) DOI: 10.1002/hyp.9773

Study on effect of surface roughness on overland flow from different geometric surfaces through numerical simulation

Sunil P. Maske Research Scholar* and Manoj K. Jain Associate Professor
Department of Hydrology, Indian Institute of Technology, Roorkee, India

Abstract:

Effect of variability in surface roughness on overland flow from different geometric surfaces is investigated using numerical solution of diffusion wave equation. Three geometric surfaces rectangular plane, converging and diverging plane at slopes 1 to 3% are used. Overland flow is generated by applying rainfall at constant intensity of 10 mm/h for period 30 min and 100 min. Three scenarios of spatial roughness conditions viz. roughness increasing in downstream direction, roughness decreasing in downstream direction and roughness distributed at random are considered. Effect of variability of roughness on overland flow in terms of depth, velocity of flow and discharge along the distance from upstream to downstream for different geometric surfaces are discussed in detail. Results from the study indicate that roughness distribution has significant effect on peak, time to peak and overall shape of the overland flow hydrograph. The peak occurs earlier for the scenario when roughness increases in downstream direction as compared to scenario when roughness is decreasing in downstream for all three geometric surfaces due to very low friction factor and more velocity at the top of the domain. The converging plane attains equilibrium state early as compared to rectangular and diverging plane. Different set of random values result in different time to peak and shape of hydrograph for rectangular and diverging plane. However, in case of converging plane, the shape of computed hydrographs remains almost similar for different sets of random roughness values indicating stronger influence of converging geometry than effect due to variation of roughness sequence on computed runoff hydrograph. Hierarchically, the influence of geometry on overland flow is stronger than the influence of slope and the influence of slope is stronger than the influence of roughness.

KEY WORDS surface roughness; rectangular plane; converging plane; diverging plane; overland flow; diffusion wave

Received 20 June 2012; Accepted 19 February 2013

INTRODUCTION

The complex geometry of a watershed can be modeled using various simplified geometric configurations. These configurations can be classified as (1) plane surface (Figure 1(a)), (2) converging surface (Figure 1(b)) (Woolhiser, 1969; Campbell *et al*., 1984) and (3) diverging surface (Figure 1(c)) (Campbell *et al*., 1984). Many small upland areas can be conveniently represented by a linearly converging geometric section. Large watersheds have subareas that can be adequately represented by a converging section (Beven, 1978). Leaf-shaped basins diverge in their upland portions and converge in their lower portions. Hence, it is necessary to model watersheds by a particular geometric section. A converging surface accounts for runoff concentration, and it provides a better representation of watershed runoff.

The converging element is a segment of a conical surface where the radius vector has a constant slope. Thus, the converging surface over which flow may occur is defined geometrically by three shape parameters length of section (R_0), a parameter related to degree of convergence (c), radial symmetry (Θ) and slope of the surface. In a converging section, flow surface does not extend to lower vortex; hence, R_0(1-c) is the length of flow. Because of radial symmetry, Θ does not affect flow characteristics on a unit width basis, and depends on R_0 and c. The parameter c varies from 0 to 1.

The diverging element is a segment of a conical surface where the radius vector has a constant slope. Thus, the diverging surface over which flow may occur is defined geometrically by three shape parameters, i.e. length of the section (R), a parameter related to the degree of divergence (a) and interior angle (Θ). In a diverging section, the flow surface does not extend to the upper vortex; hence, R(1-a) is the length of flow. Because of radial symmetry, Θ does not affect flow characteristics on a unit width basis and depends on R and a. The divergence parameter 'a' varies from 0 to 1. If a = 1, the surface will become a rectangular plane. Therefore, 'a' is an inverse measure of divergence. Method to construct a diverging surface from a

*Correspondence to: Sunil P. Maske, Department of Hydrology, Indian Institute of Technology, Roorkee, India
Email: sunilmaske@yahoo.co.in

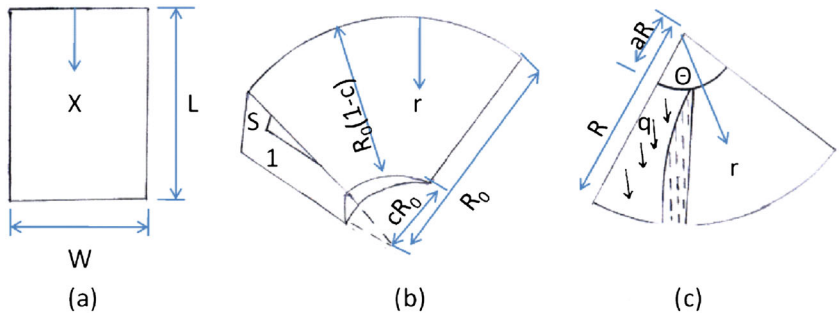

Figure 1. Geometric surfaces: (a) rectangular plane, (b) converging section and (c) diverging section

topographic map of a basin is described by Agiralioglu and Singh (1980). The diverging section possesses some interesting features: (1) its response is similar to that of a cascade of planes of decreasing size; (2) its discrete analogue is a system composed of unequal nonlinear reservoirs used in parametric hydrology.

Unsteady flow in open channels and overland planes of different geometric configurations can be described by a set of hyperbolic partial differential equations commonly known as St. Venant equations (Chow, 1959). These equations describe the conservation of mass and momentum in terms of the partial derivatives of the dependent variables. Because of the presence of nonlinear terms, a closed-form solution of these equations is not available, except for very simplified cases. A close scrutiny of present-day hydrologic models indicate that simplified forms of St. Venant equations specially kinematic and diffusion wave approximation have been used widely for simulating overland flow and channel flow from watersheds (Nejafi, 2003; Jain *et al.*, 2004; Tsai and Yang, 2005; Melek and Medina, 2007). Excellent review of popular models is given in Singh and Woolhiser (2002); Singh and Frevert (2002).

Woolhiser (1969) solved the characteristic equations of kinematic flow on a converging surface numerically. Singh and Woolhiser (1976) reported a kinematic converging flow model for watershed runoff and verified it with the field data. Campbell *et al.* (1984) proposed a similarity solution for the kinematic equations of converging flow. Moore (1985) approximated the behavior of converging and diverging surfaces by defining the nature of the outflow hydrograph and the shape of the water surface profile for constant and time varying rainfall excess. The analytical solution for the flow over converging plane using the method of characteristics is given by Singh (1996). A survey of literature indicates that overland flow on diverging surfaces has seldom been explicitly included in mathematical modeling of basin runoff. Yu and McNown (1964), Langford and Turner (1973) applied diverging flow model to a number of events on impervious surfaces.

Wu *et al.* (1978, 1982) examined the effects of spatial variability of roughness on runoff hydrograph from an experimental watershed facility and found that under certain conditions an equivalent uniform roughness could be used for a watershed with non-uniform roughness. Lehrsch *et al.* (1987, 1988) determined the spatial variation of eight physically significant roughness indices using a semi-variogram analysis. Hairsine and Parlange (1986) demonstrated the formation of kinematic shocks on various surfaces with different degree of roughness and analyzed the error incurred when curved surface was represented by a kinematic cascade model. Vieux and Farajalla (1994) evaluated the error resulting from smoothing the hydraulic roughness coefficients in modeling overland flow with finite element solution and revealed an almost Brownian variation of roughness coefficients. Huang and Lee (2009) analyzed the effects of spatially distributed roughness on flow hydrographs and concluded that runoff behavior is significantly influenced not only by the spatial distribution of roughness but also by range of variability of roughness. Hydraulically, the value of roughness should be dependent on the interactions between surface and the flow only (Wong, 1997).

The present study is undertaken to analyze the runoff characteristics in relation to spatial variability of roughness for rectangular, converging and diverging planes using numerical experiments. Such a comparison is perhaps not available in literature. For conducting numerical experiments, numerical solution of diffusion wave equation is used to simulate runoff hydrograph resulting due to application of rainfall at a constant rate of 10 mm/h for durations of 30 min and 100 min on rectangular, converging and diverging planes. The duration of the storm is selected in such a way that for a time duration of 100 min, the time to equilibrium discharge is reached for all studied geometric planes whereas for the other duration (i.e. 30 min), time to equilibrium discharge has not reached for most of cases. These two durations are selected to understand the overland flow characteristics with equilibrium and non-equilibrium discharge cases from different

DOI: 10.1002/hyp

geometric configurations. The slope of the planes varied between 1 and 3%.

GOVERNING EQUATIONS

The overland and channel flows can be modeled by approximations of the St. Venant equations of continuity and momentum (Chaudhry, 1993). Studies conducted in past have demonstrated that the diffusion wave approximation of the full St. Venant equations is appropriate for many cases of practical interest (Gonwa and Kavvas, 1986; Ponce, 1989; Jain and Singh, 2005). Govindaraju *et al*. (1990) and Singh (1996) have shown that in many cases, the dynamic wave and diffusion wave approximations give equally good representation of the St. Venant equation when used for overland flow routing. Singh and Aravamuthan (1997, 1998) investigated the accuracy of the diffusion wave approximation in comparison with the St. Venant equations for a variety of cases and found that diffusion wave approximation is sufficiently accurate for modeling over land flow as well as channel flow. Therefore, in the present study, a one-dimensional solution of the diffusion wave approximation of the St. Venant equation is used to describe overland flow over different geometric surfaces. The one-dimensional diffusion wave equations in conservative form for shallow water flow are written in vector notations as (Chaudhry, 1993).

$$U_t + F_x = S \tag{1}$$

Where,

$$U = \begin{pmatrix} h \\ 0 \end{pmatrix} \tag{2}$$

$$F = \begin{pmatrix} q \\ h \end{pmatrix} \tag{3}$$

For rectangular plane

$$S = \begin{pmatrix} i_e \\ S_0 - S_f \end{pmatrix} \tag{4}$$

For converging section

$$S = \begin{pmatrix} i_e - \dfrac{q}{R_0 - r} \\ S_0 - S_f \end{pmatrix} \tag{5}$$

For diverging section

$$S = \begin{pmatrix} i_e - \dfrac{q}{r} \\ S_0 - S_f \end{pmatrix} \tag{6}$$

Where h is flow depth, q is the discharge per unit width, x is distance along the flow direction for rectangular plane, r is distance along the flow direction for converging and diverging plane, t is time coordinate, i_e is the effective rainfall, S_0 is bed slope and S_f is friction slope, R_0 is radius of converging section.

The friction slope S_f is approximated as (Chow, 1959; Chaudhry, 1993)

$$S_f = \frac{n^2 u^2}{h^{4/3}} \tag{7}$$

Where n is Manning's roughness coefficient, and u is velocity of the flow.

NUMERICAL SOLUTION

The governing differential equations described above are solved numerically using the MacCormack scheme (MacCormack, 1969). It is a two-step predictor corrector scheme, second-order accurate in space and time and has the capability of capturing the shocks without isolating them (Chaudhry, 1993). This scheme has been used by Fennema and Chaudhry (1986, 1987); Dammuller *et al*. (1989); Jain and Singh (2005) and many others. In the first alternative, backward finite differences are used to approximate the spatial partial derivatives in the predictor

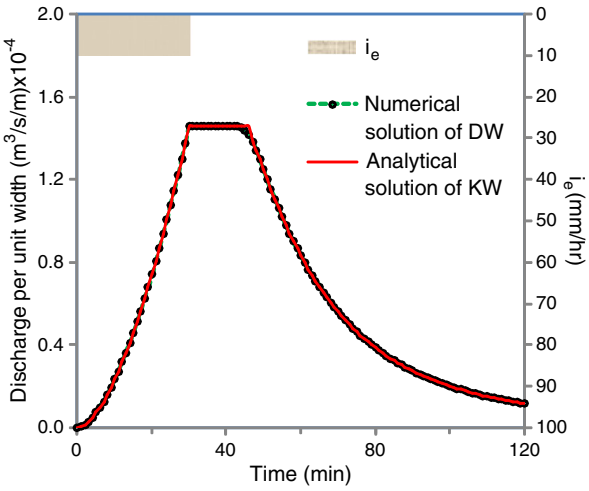

Figure 2. Comparison of analytical and numerical solution (td = 30 min)

DOI: 10.1002/hyp

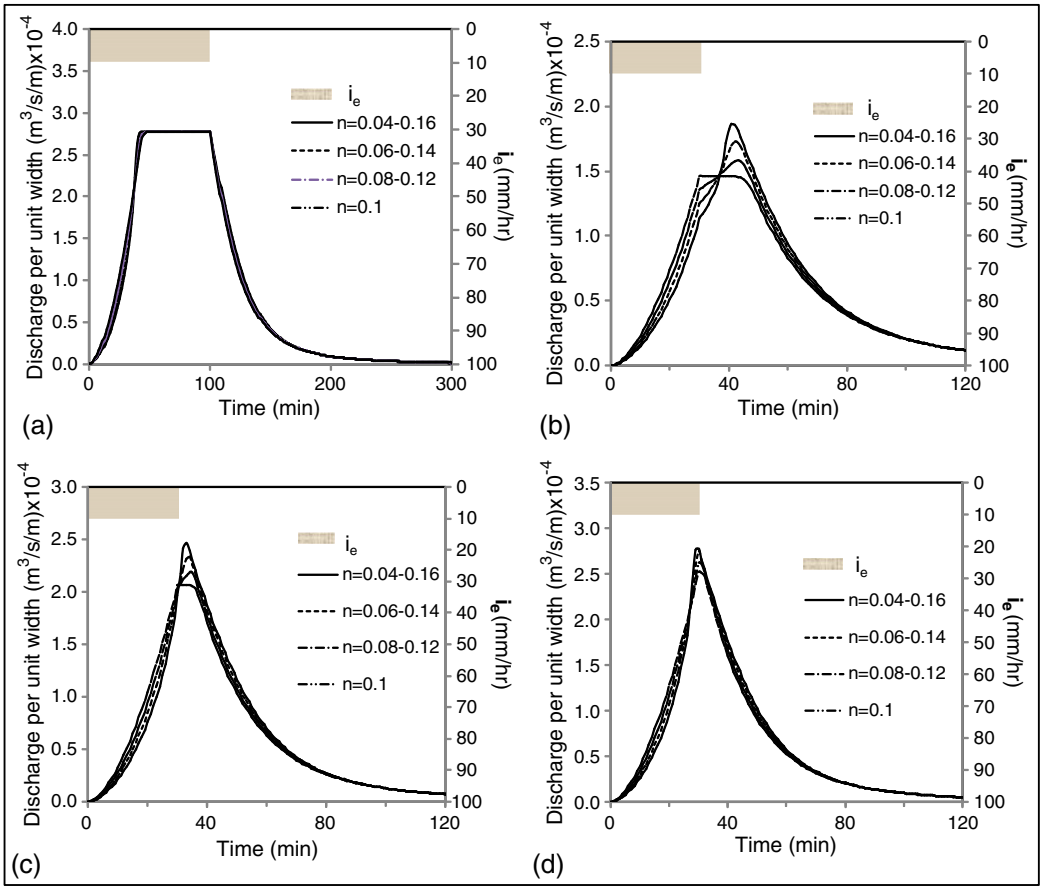

Figure 3. Hydrographs (rectangular plane) for roughness increasing in downstream direction for different slope ((a) for slope 0.01 and td = 100 min, (b) for slope 0.01 and td = 30 min, (c) for slope 0.02 and td = 30 min and (d) for slope 0.03 and td = 30 min)

part, and forward finite differences are utilized in the corrector part. The values of variables determined during the predictor part are used during the corrector part. In the second alternative, forward finite differences are used in the predictor part, and backward finite differences are used in the corrector part. The direction of differencing from one time step to next is alternated (Chaudhry, 1993).

Alternative 1

Predictor.

$$\frac{\partial U}{\partial t} = \frac{U_i^* - U_i^k}{\Delta t} \tag{8}$$

$$\frac{\partial F}{\partial x} = \frac{F_{i+1}^k - F_i^k}{\Delta x} \tag{9}$$

Where, *represents variables computed during the predictor step, t is time, x is distance, i is space node number, k is time node number, Δx is space interval for flow routing and Δt is time interval for flow routing. Substituting these finite difference approximations into Equation (1) results in

$$U_i^* = U_i^k - \frac{\Delta t}{\Delta x}\left(F_{i+1}^k - F_i^k\right) - S_i^k \Delta t \tag{10}$$

Table I. Hydrograph characteristics for rectangular plane for roughness increasing in downstream direction

Slope (m/m)	Roughness range	td = 100 min		td = 30 min	
		q_p (m^2/s/m)	t_p (min)	q_p (m^2/s/m)	t_p (min)
0.01	0.1 (uniform)	2.778×10^{-4}	47	1.46×10^{-4}	30
	0.04–0.16	2.778×10^{-4}	44	1.87×10^{-4}	41
	0.06–0.14	2.778×10^{-4}	45	1.73×10^{-4}	42
	0.08–0.12	2.778×10^{-4}	46	1.59×10^{-4}	43
0.02	0.1 (uniform)	2.778×10^{-4}	37	2.06×10^{-4}	30
	0.04–0.16	2.778×10^{-4}	34	2.47×10^{-4}	33
	0.06–0.14	2.778×10^{-4}	35	2.33×10^{-4}	34
	0.08–0.12	2.778×10^{-4}	36	2.19×10^{-4}	34
0.03	0.1 (uniform)	2.778×10^{-4}	33	2.53×10^{-4}	30
	0.04–0.16	2.778×10^{-4}	29	2.77×10^{-4}	29
	0.06–0.14	2.778×10^{-4}	31	2.76×10^{-4}	30
	0.08–0.12	2.778×10^{-4}	32	2.63×10^{-4}	30

DOI: 10.1002/hyp

It gives the predictor value of depth (h^*) from which the predictor value of discharge per unit width (q^*) is calculated for use in the corrector step.

Corrector.

$$\frac{\partial U}{\partial t} = \frac{U_i^{**} - U_i^k}{\Delta t} \tag{11}$$

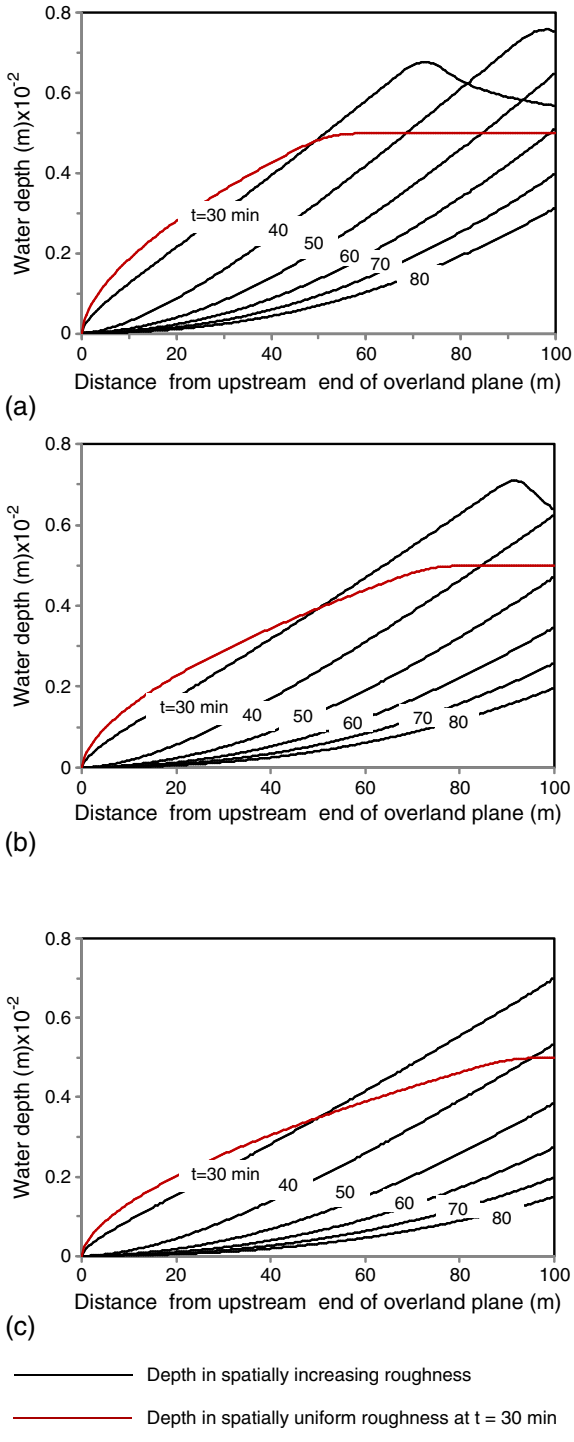

Figure 4. Water depth along the flow direction of the overland plane (rectangular plane) for increasing roughness (0.04–0.16) at slope 0.01 (a), 0.02 (b) and 0.03 (c), td = 30 min

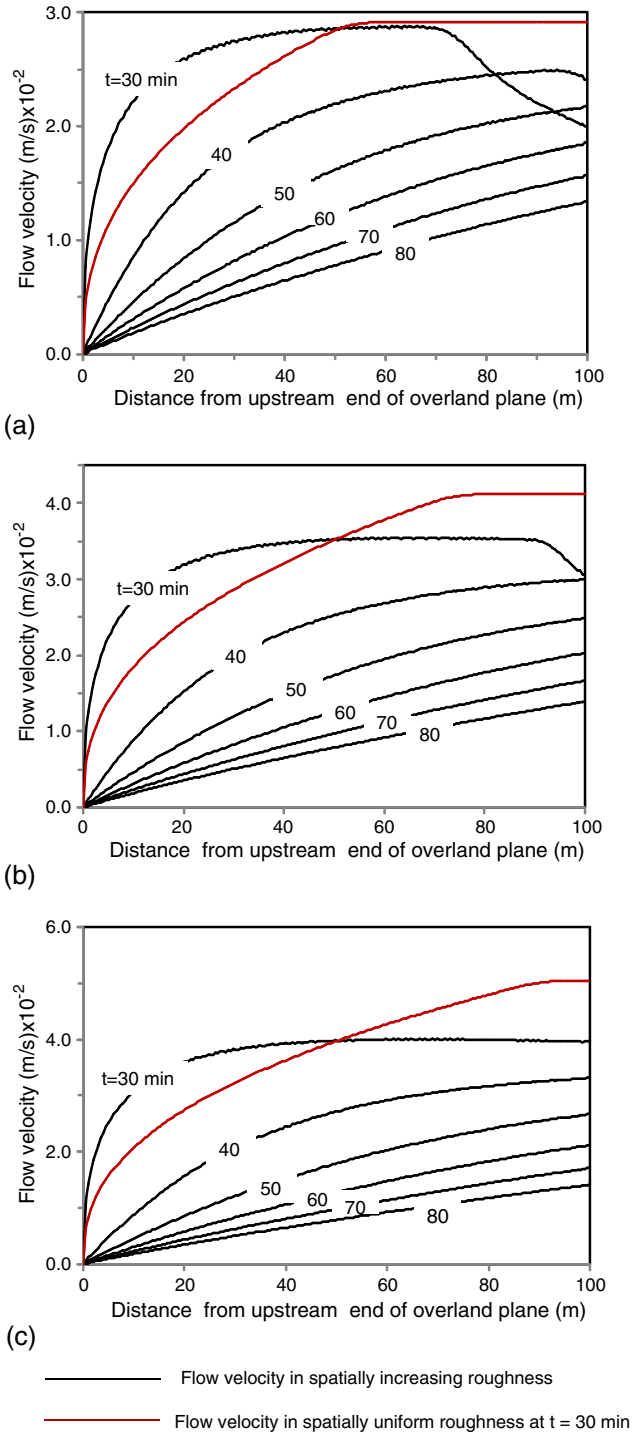

Figure 5. Flow velocity along the flow direction of the overland plane (rectangular plane) for increasing roughness (0.04–0.16) at slope 0.01(a), 0.02 (b) and 0.03 (c), td = 30 min

DOI: 10.1002/hyp

$$\frac{\partial F}{\partial x} = \frac{F_i^k - F_{i-1}^k}{\Delta x} \quad (12)$$

$$U_i^{**} = U_i^k - \frac{\Delta t}{\Delta x}\left(F_i^* - F_{i-1}^*\right) - S_i^* \Delta t \quad (13)$$

Substituting above finite differences and S = S^* in Equation (1), we obtain

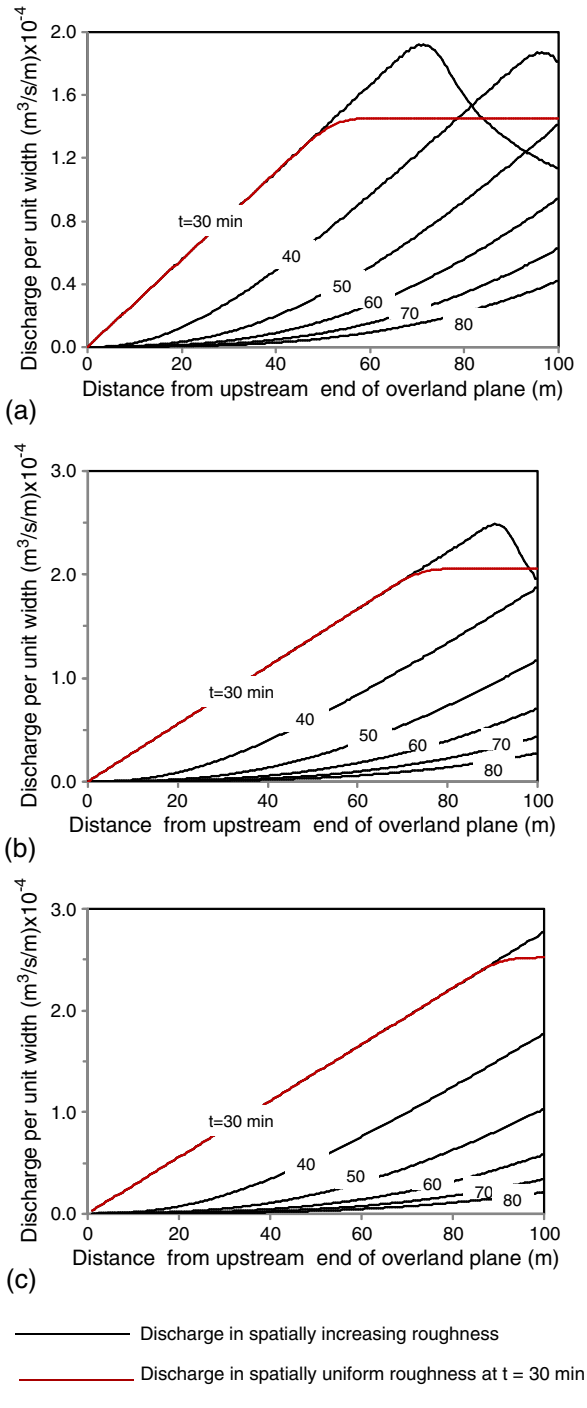

Figure 6. Discharge along the flow direction of the overland plane (rectangular plane) for increasing roughness (0.04–0.16) at slope 0.01(a), 0.02 (b) and 0.03 (c), td = 30 min

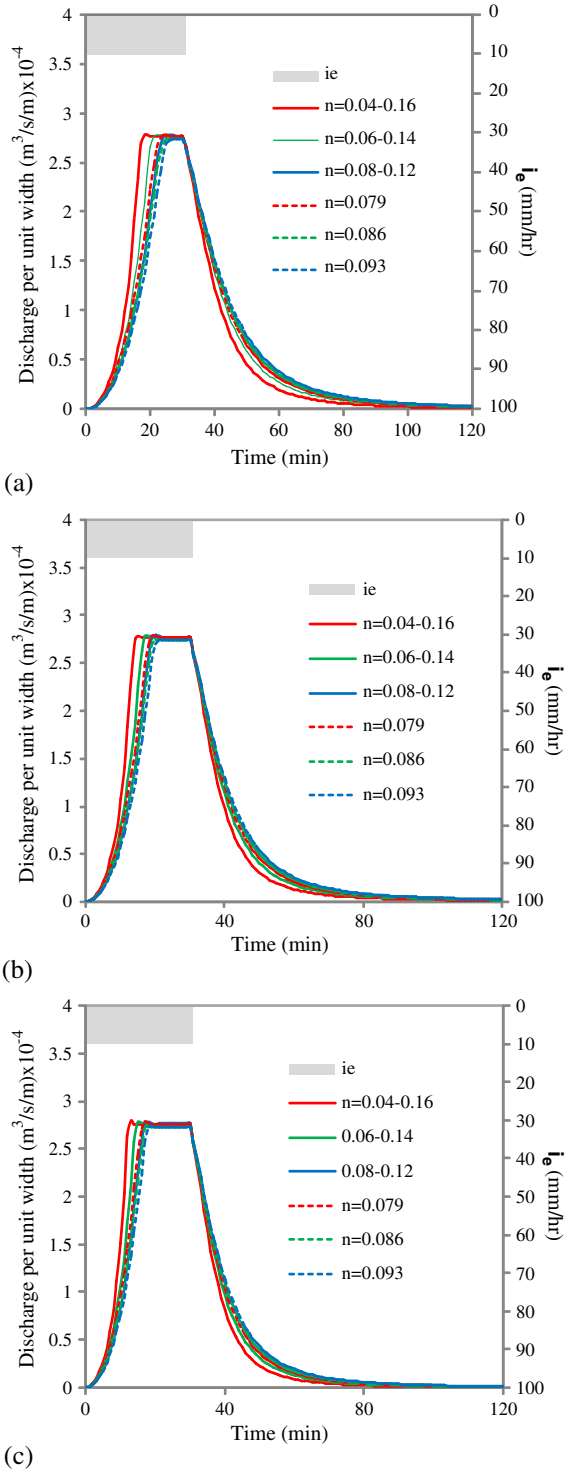

Figure 7. Hydrographs for scenario1 for converging plane ((a) for s = 0.01, (b) for s = 0.02 and (c) for s = 0.03) td = 30 min

DOI: 10.1002/hyp

Where, ** represents variables computed during the corrector part.

Alternative 2

Predictor.

$$\frac{\partial U}{\partial t} = \frac{U_i^* - U_i^k}{\Delta t} \tag{14}$$

$$\frac{\partial F}{\partial x} = \frac{F_i^k - F_{i-1}^k}{\Delta x} \tag{15}$$

Substituting these finite differences into Equation (1) and simplification of resulting equation yields

$$U_i^* = U_i^k - \frac{\Delta t}{\Delta x}\left(F_i^k - F_{i-1}^k\right) - S_i^k \Delta t \tag{16}$$

It gives the predictor value of depth (h^*) from which of the predictor value of discharge per unit width (q^*) is calculated for use in the corrector step.

Corrector.

$$\frac{\partial U}{\partial t} = \frac{U_i^{**} - U_i^k}{\Delta t} \tag{17}$$

$$\frac{\partial F}{\partial x} = \frac{F_{i+1}^k - F_i^k}{\Delta x} \tag{18}$$

Table II. Characteristics of hydrograph for converging plane for roughness increasing in downstream direction

Slope (m/m)	Roughness range	td = 100 min		td = 30 min	
		q_p (m^2/s/m)	t_p (min)	q_p (m^2/s/m)	t_p (min)
0.01	0.04–0.16	2.778×10^{-4}	18	2.778×10^{-4}	18
	0.079 (uniform)	2.778×10^{-4}	25	2.778×10^{-4}	25
	0.06–0.14	2.778×10^{-4}	21	2.778×10^{-4}	21
	0.086 (uniform)	2.778×10^{-4}	26	2.778×10^{-4}	26
	0.08–0.12	2.778×10^{-4}	25	2.778×10^{-4}	25
	0.093 (uniform)	2.778×10^{-4}	28	2.778×10^{-4}	28
0.02	0.04–0.16	2.778×10^{-4}	15	2.778×10^{-4}	15
	0.079 (uniform)	2.778×10^{-4}	19	2.778×10^{-4}	19
	0.06–0.14	2.778×10^{-4}	17	2.778×10^{-4}	17
	0.086 (uniform)	2.778×10^{-4}	20	2.778×10^{-4}	20
	0.08–0.12	2.778×10^{-4}	20	2.778×10^{-4}	20
	0.093 (uniform)	2.778×10^{-4}	21	2.778×10^{-4}	21
0.03	0.04–0.16	2.778×10^{-4}	14	2.778×10^{-4}	14
	0.079 (uniform)	2.778×10^{-4}	17	2.778×10^{-4}	17
	0.06–0.14	2.778×10^{-4}	15	2.778×10^{-4}	15
	0.086 (uniform)	2.778×10^{-4}	18	2.778×10^{-4}	18
	0.08–0.12	2.778×10^{-4}	17	2.778×10^{-4}	17
	0.093 (uniform)	2.778×10^{-4}	19	2.778×10^{-4}	19

Substituting above finite differences and $S = S^*$ in Equation (1), we obtain

$$U_i^{**} = U_i^k - \frac{\Delta t}{\Delta x}\left(F_{i+1}^* - F_i^*\right) - S_i^* \Delta t \tag{19}$$

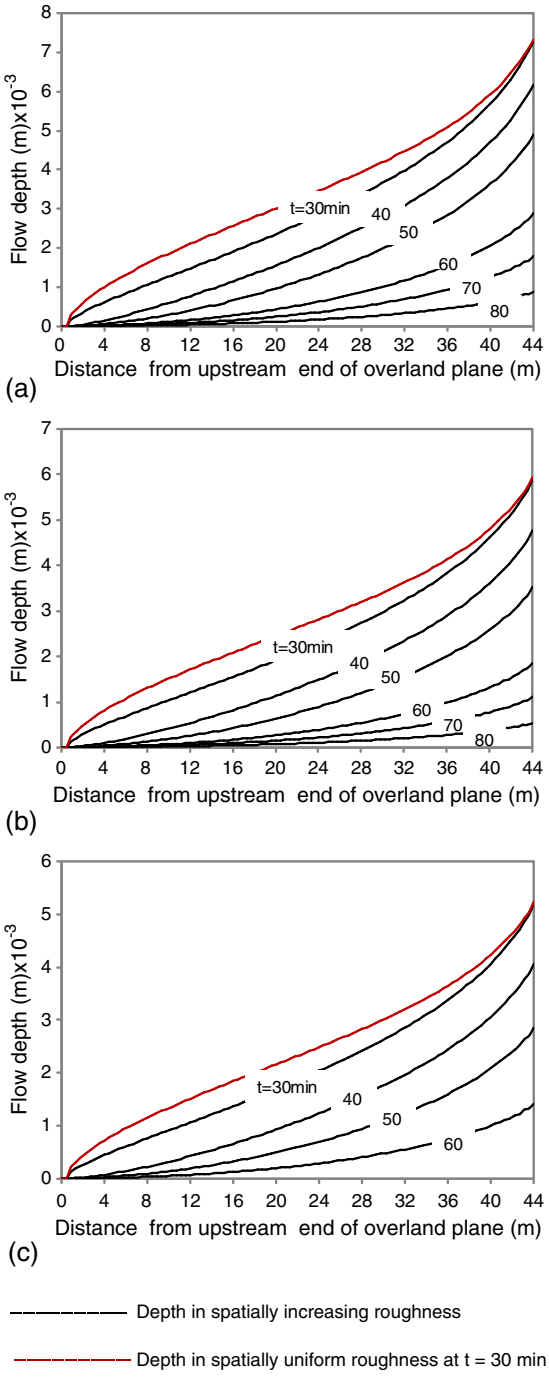

Figure 8. Water depth along the flow direction of the converging plane for increasing roughness (0.04–0.16) at slope 0.01 (a), 0.02 (b) and 0.03 (c), td = 30 min

DOI: 10.1002/hyp

The value of U_i at the next time step is given by

$$U_i^{k+1} = \frac{U_i^* + U_i^{**}}{2} \tag{20}$$

For numerical stability of the scheme, a Courant–Friedrichs–Lewy (CFL) criterion is used. The CFL criterion is a necessary condition for convergence of numerical solution of certain partial differential equations while solving them numerically using explicit finite difference scheme (Chaudhry, 1993). For stability of

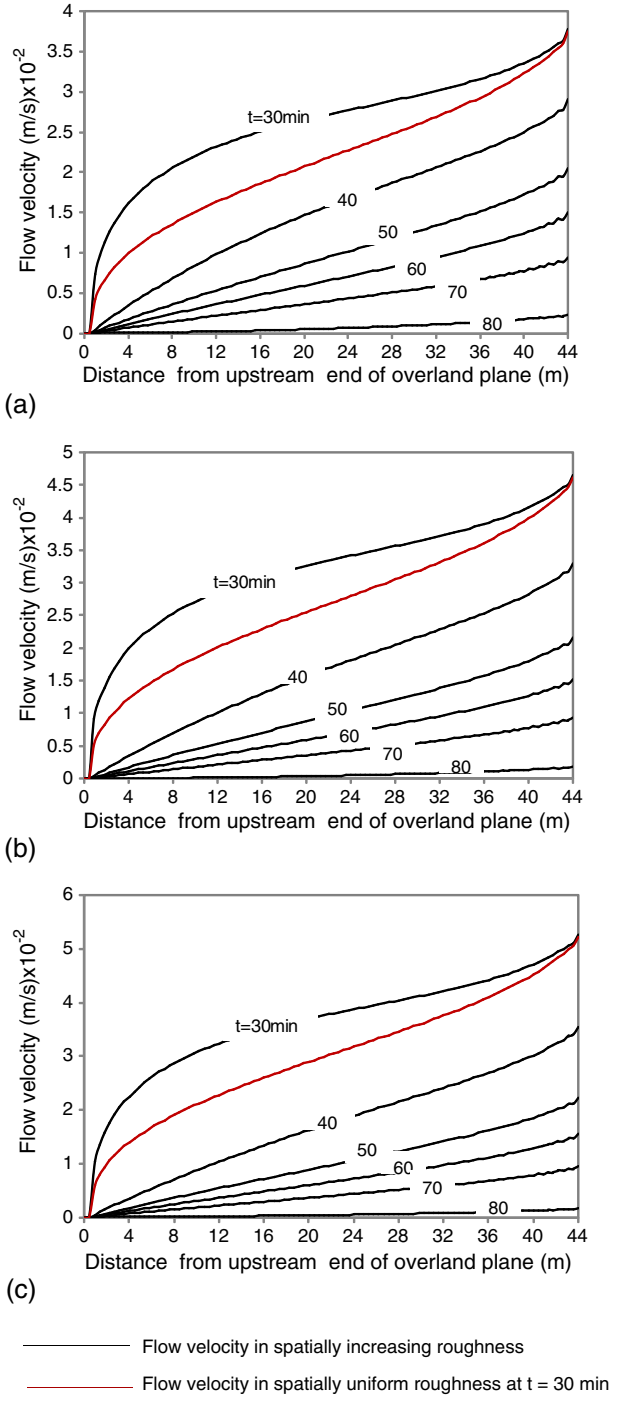

Figure 9. Flow velocity along the flow direction of the converging plane for increasing roughness (0.04–0.16) at slope 0.01(a), 0.02 (b) and 0.03 (c), td = 30 min

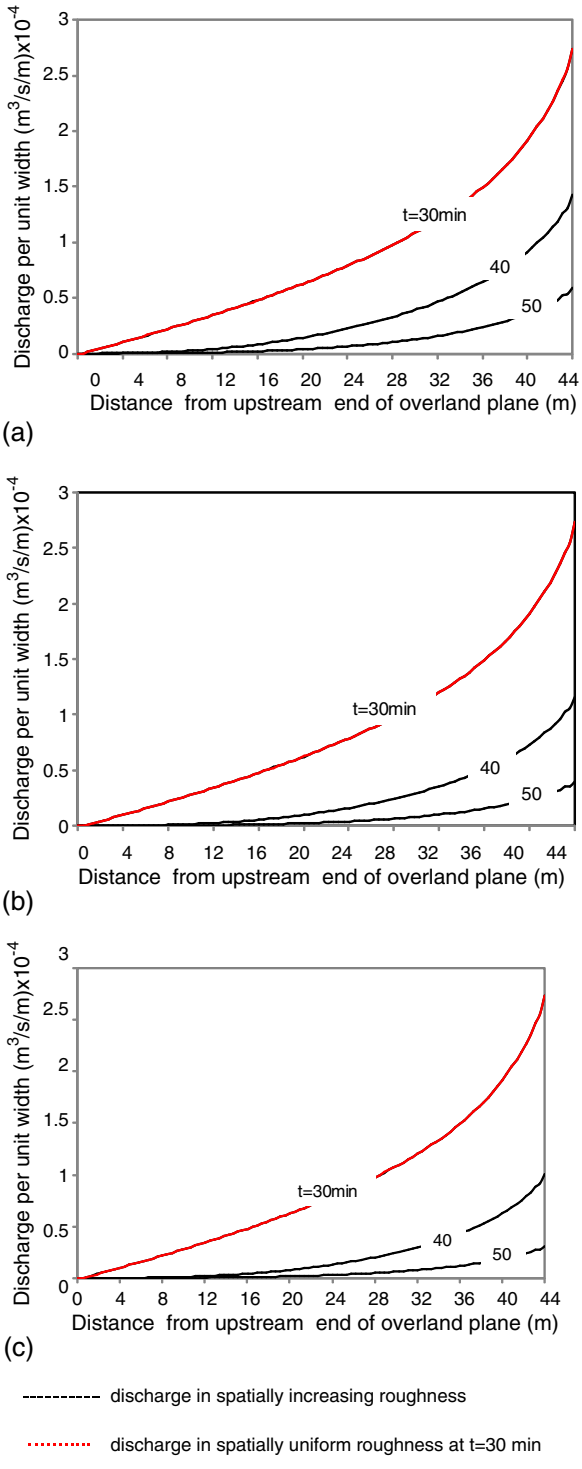

Figure 10. Discharge along the flow direction of the converging plane for increasing roughness (0.04–0.16) at slope 0.01(a), 0.02 (b) and 0.03 (c), td = 30 min

DOI: 10.1002/hyp

explicit finite difference scheme, the grid speed $\Delta x/\Delta t$ must be greater than wave speed. In other words, a stable condition means that any wave within the solution domain should not cross a distance greater than Δx in time step interval Δt.

$$max\left(\frac{(u+\sqrt{gh})\Delta t}{\Delta x}\right)\leq 1 \tag{21}$$

Where, g is acceleration due to gravity.

Initial condition

(a) For rectangular plane

The depth at the space node for the most upstream node and the flow depth at start are assumed to be zero.

$$h(i,0)=0.0 \tag{22}$$

where i is space node, 0 indicates time node at time = 0.

(b) for converging section

$$h(i,0)=0.0 \tag{23}$$

$$h(0,k)=0.0 \tag{24}$$

0 indicates most upstream space node and k is time node

(c) for diverging section

$$h(i,0)=0.0 \tag{25}$$

$$h(aR,k)=0.0 \tag{26}$$

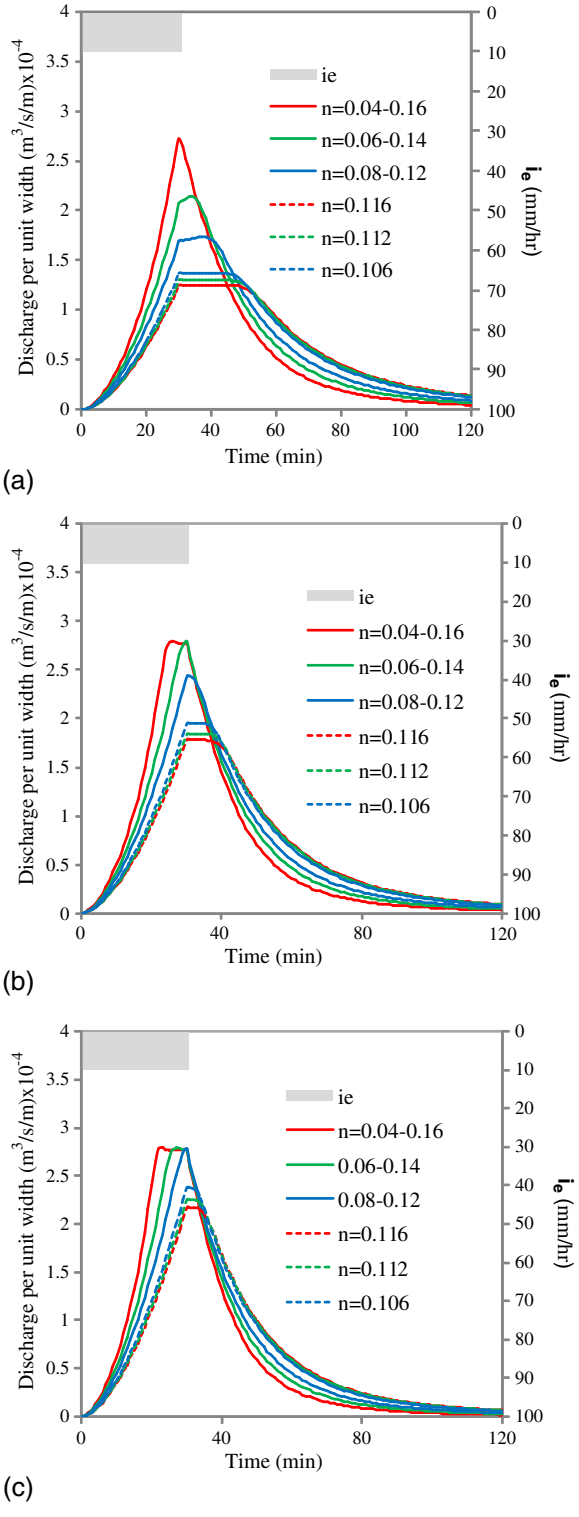

Figure 11. Hydrographs for scenario 1 for diverging plane ((a) for s = 0.01, (b) for s = 0.02 and (c) for s = 0.03), td = 30 min

Table III. Hydrograph characteristics for diverging plane for roughness increasing in downstream direction

Slope (m/m)	Roughness range	td = 100 min		td = 30 min	
		q_p (m^2/s/m)	t_p (min)	q_p (m^2/s/m)	t_p (min)
0.01	0.04–0.16	$2.778x10^{-4}$	32	$2.73x10^{-4}$	30
	0.116 (uniform)	$2.778x10^{-4}$	52	$1.258x10^{-4}$	30
	0.06–0.14	$2.778x10^{-4}$	37	$2.15x10^{-4}$	33
	0.112 (uniform)	$2.778x10^{-4}$	51	$1.303x10^{-4}$	30
	0.08–0.12	$2.778x10^{-4}$	42	$1.74x10^{-4}$	36
	0.106 (uniform)	$2.778x10^{-4}$	49	$1.377x10^{-4}$	30
0.02	0.04–0.16	$2.778x10^{-4}$	25	$2.778x10^{-4}$	25
	0.116 (uniform)	$2.778x10^{-4}$	41	$1.779x10^{-4}$	30
	0.06–0.14	$2.778x10^{-4}$	26	$2.778x10^{-4}$	26
	0.112 (uniform)	$2.778x10^{-4}$	40	$1.842x10^{-4}$	30
	0.08–0.12	$2.778x10^{-4}$	30	$2.778x10^{-4}$	30
	0.106 (uniform)	$2.778x10^{-4}$	39	$1.947x10^{-4}$	30
0.03	0.04–0.16	$2.778x10^{-4}$	23	$2.778x10^{-4}$	23
	0.116 (uniform)	$2.778x10^{-4}$	36	$2.178x10^{-4}$	30
	0.06–0.14	$2.778x10^{-4}$	26	$2.778x10^{-4}$	26
	0.112 (uniform)	$2.778x10^{-4}$	35	$2.256x10^{-4}$	30
	0.08–0.12	$2.778x10^{-4}$	30	$2.778x10^{-4}$	30
	0.106 (uniform)	$2.778x10^{-4}$	34	$2.384x10^{-4}$	30

DOI: 10.1002/hyp

where, a is parameter related to degree of divergence, and R is length of the section.

Boundary condition

At downstream end, the depth gradient is assumed to be zero (Morris, 1979; Tayfur *et al*., 1993; Wang and Hjelmfelt, 1998). The zero depth gradient condition can be written as

$$h(N,k) = h(N+1,k) \tag{27}$$

where, N is total number of space nodes.

Description of numerical experiments for different roughness scenarios

A computer code in FORTRAN 77 is developed to solve governing differential equation described above using MacCormack predictor corrector scheme. To test the correctness of the developed computer code for numerical solution of diffusion wave equations, the results obtained from the developed code is compared with those obtained using analytical solution of kinematic wave equation for an impervious rectangular plane of 1 m width and 100 m length. The hydrograph obtained by numerical solution of the diffusion wave equations using MacCormack scheme and that obtained

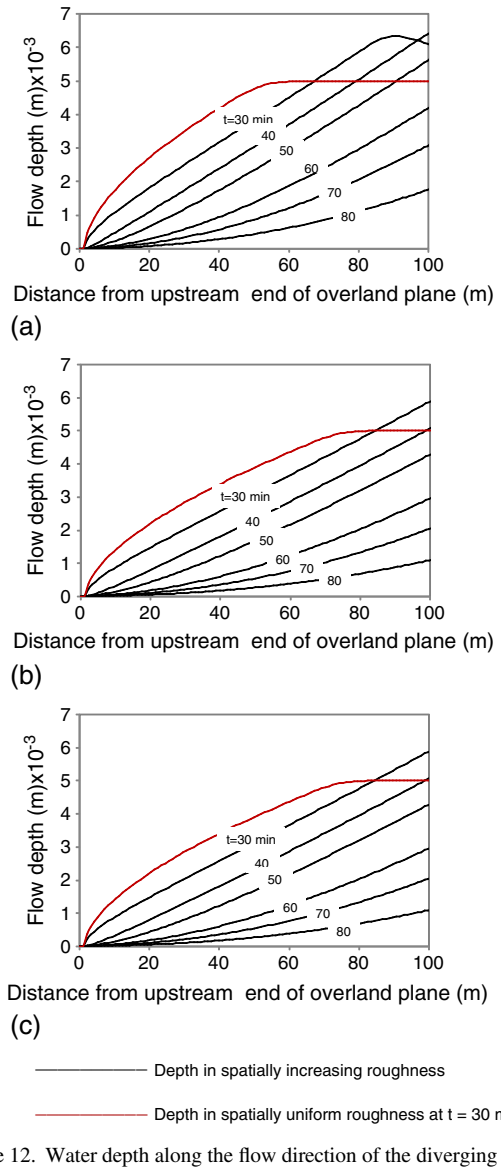

Figure 12. Water depth along the flow direction of the diverging plane for increasing roughness (0.04–0.16) at slope 0.01 (a), 0.02 (b) and 0.03 (c), td = 30 min

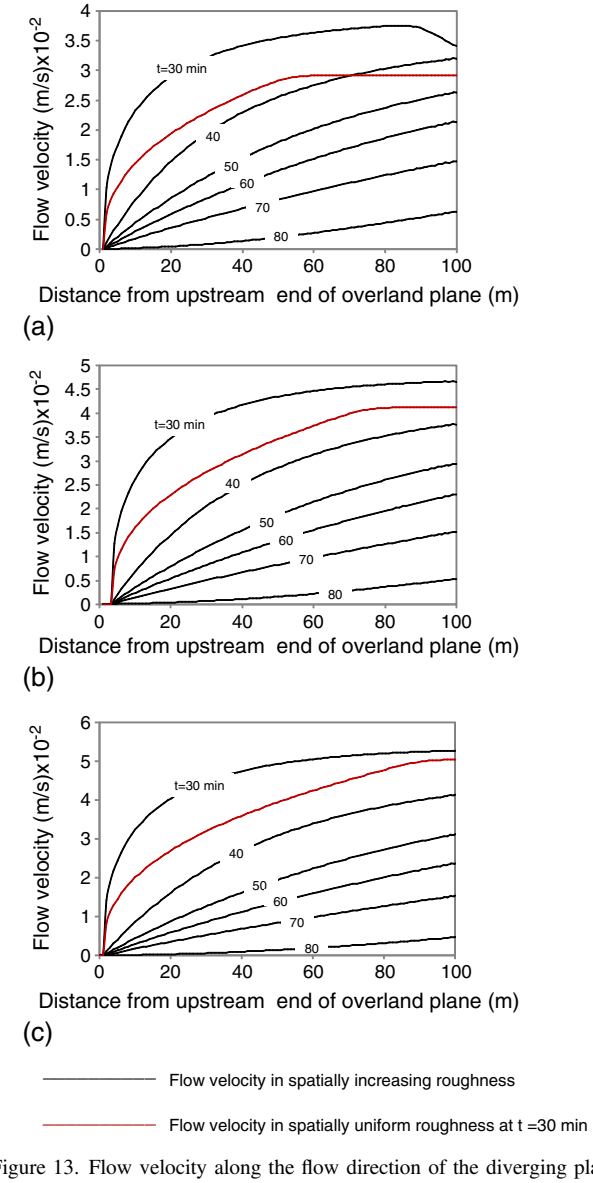

Figure 13. Flow velocity along the flow direction of the diverging plane for increasing roughness (0.04–0.16) at slope 0.01(a), 0.02 (b) and 0.03 (c), td = 30 min

DOI: 10.1002/hyp

by analytical solution (Henderson and Wooding, 1964) for constant rainfall intensity of 10 mm/h for 30 min duration at 1% slope of the overland plane is depicted in Figure 2. As can be seen from Figure 2, the hydrograph computed using developed computer code and that obtained using analytical solution are identical. The ratio of total volume of runoff generated to the total volume of applied rainfall found to be unity which implies mass conservation. The developed computer code is therefore suitable for further numerical experiments with respect to spatial roughness variation for different conditions.

To explore the effect of variability of roughness on computed runoff hydrograph from different geometric surfaces, three scenarios for roughness variation are considered. These are, (1) roughness increasing in downstream direction, (2) roughness decreasing in downstream direction and (3) roughness distributed at random along the surface. For scenario (1) and (2), the range of variability of Manning's roughness (linear increase or decrease) along the flow direction investigated are between 0.04 – 0.16, 0.06 – 0.14 and 0.08 – 0.12.The value of the roughness is increased or decreased in linear step of 1/200 along the direction of flow. For scenario 3, the random roughness values in the range 0.04 to 0.16 are generated for use in simulation of overland flow. The range of Manning's roughness between 0.04 and 0.16 is chosen because in natural watersheds, the variability of Manning's roughness for different land use classes is generally professed within these ranges. For fallow land with no residue, the Manning's roughness may be of order of 0.05, and for short rigid grass, it could be as high as 0.16 (Chow, 1959; Engman, 1986; Shen and Julien, 1992). Resultant hydrographs obtained from variable roughness scenarios are compared with those obtained using weighted areal average values of roughness for different roughness ranges and scenarios. The weighted areal average value of roughness is computed as

$$\text{weighted areal average roughness} = \frac{\sum area\ of\ segment\ \ x\ assigned\ value\ of\ n\ to\ the\ segment}{total\ area\ of\ plane} \tag{28}$$

Using Equation (28), weighted areal average roughness for rectangular plane is 0.1 for all three roughness ranges studied. For converging and diverging sections, the weighted areal roughness values vary with range of roughness variation considered and its increment or decrement with respect to direction of flow, and the same is reported in subsequent tables.

The dimension of an impervious rectangular plane considered for the present study is 100 m × 1 m. The dimensions of converging and diverging plane are chosen such that their area is preserved (100 m^2). In the present study, R_o is taken as 49 m, and c is taken as 0.1 for converging section, and divergence parameter 'a' is taken as 0.057, and R is taken as 108 m for diverging section.

Scenario – 1: Roughness increasing in the downstream direction

(a) Rectangular plane

The computed hydrographs due to application of constant rainfall at 10 mm/h for 100 and 30 min durations of rainfall (td) are shown in Figure 3 for different slopes of rectangular plane. Information about peak and time to peak discharge for different rain durations, slopes and roughness ranges studies is listed in Table I. For td = 100 min, hydrograph attained temporal equilibrium state for given slopes, but for td = 30 min, all hydrographs rose and recessed successively without experiencing temporal equilibrium state with exception of n = 0.04 – 0.16 for slope 0.03. Compared to spatial uniform roughness condition for td = 30 min, the computed peak discharge is 28.1% more when roughness is increased in downstream direction in range 0.04 – 0.16 on overland plane slope of 0.01, whereas for slope 0.02 and 0.03, it is 19.9% and 9.8%, respectively. For td > time of concentration (tc), the hydrograph shape is identical for all ranges. The rising limb of hydrograph is steeper in case when roughness in increasing in downstream direction as compared to case for hydrograph computed using equivalent weighted areal average roughness. The shape of the computed hydrograph is dependent on roughness variability for different slopes for rainfall duration less than time of concentration. In general, the peak discharge increases as slope increases for all roughness ranges studied. As the slope of the overland flow plane increases, value of peak rate of runoff computed using different roughness ranges tends to come closer. For $t_p < tc$, peak discharge increases as slope increases. Also, peak discharge is more for larger roughness range, i.e. 0.04 – 0.16. For a particular slope,

DOI: 10.1002/hyp

change in range of roughness affects the computed peak discharge.

Depth, velocity and discharge profile

The depth, velocity of flow and discharge at different distances along downstream direction for increasing roughness in the range 0.04 – 0.16 and for slopes of overland flow planes equal to 0.01, 0.02 and 0.03 are shown in Figures 4, 5 and 6, respectively. At t = 30 min, the depth arrived at using spatially variable roughness is more than that obtained using uniform roughness condition after 60 min of simulation for slope 0.01, 50 min for slopes 0.02 and 0.03. For overland plane slope of 0.03, the depth increases towards the downstream direction. As can be seen from Figure 5, the velocity of flow decreases near outlet for slope of overland flow plane 0.01 at simulation time of 30 min and 40 min, for slope 0.02, it decreases at simulation time of 30 min. As slope of the overland plane increases, the velocity of flow for simulation time between 40 and 80 min increases towards downstream direction. At simulation time of 30 min and 40 min, discharge decreases near downstream outlet for slope of the overland plane 0.01, and for slope 0.02, it decreases at simulation time of 30 min as slope increases towards downstream direction. Similar trends of depth, velocity and discharge profiles are found when roughness is varied in ranges 0.06 – 0.14 and 0.08 – 0.12.

(b) Converging plane

The runoff hydrographs produced due to application of uniform rainfall of 10 mm/h for duration of 30 min from the converging plane for roughness increasing towards downstream direction for different slopes are shown in Figure 7. Table II shows information related to hydrographs obtained from converging plane for equivalent spatially uniform roughness as well as for roughness increasing in downstream direction for different slopes of plane and duration of rainfall. It can be seen from Table II that hydrograph rose and receded successively and attained temporal equilibrium state for td 100 min and 30 min for all slopes studied herein. The time to peak on converging plane is much less than on rectangular plane for similar slope and roughness conditions. As can be seen from Figure 7 that due to convergence of overland flow plane, the attainment of equilibrium discharge is quicker irrespective of range and variability of roughness considered in comparison to rectangular plane of similar slope. Also, the recession limb of the hydrograph recedes faster compared to that obtained on rectangular plane for similar slopes. At outlet, the flow is converging in very small area resulting in large depth of flow.

Depth, velocity and discharge profile

Figures 8, 9 and 10 depict depth, velocity and discharge at distance from the upstream end of the plane along the downstream direction resulting due to application of uniform rainfall of 10 mm/h for duration of 30 min on converging plane for roughness increasing in downstream direction. Depth as well as velocity increases as distance from the upstream end of

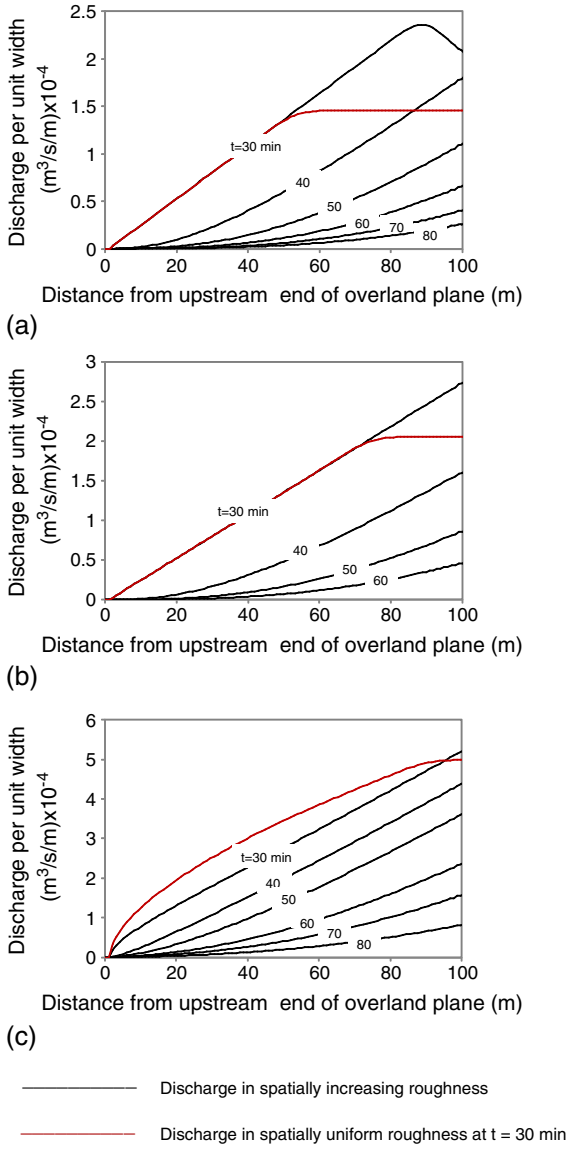

Figure 14. Discharge along the flow direction of the diverging plane for increasing roughness (0.04–0.16) at slope 0.01(a), 0.02 (b) and 0.03 (c), td = 30 min

DOI: 10.1002/hyp

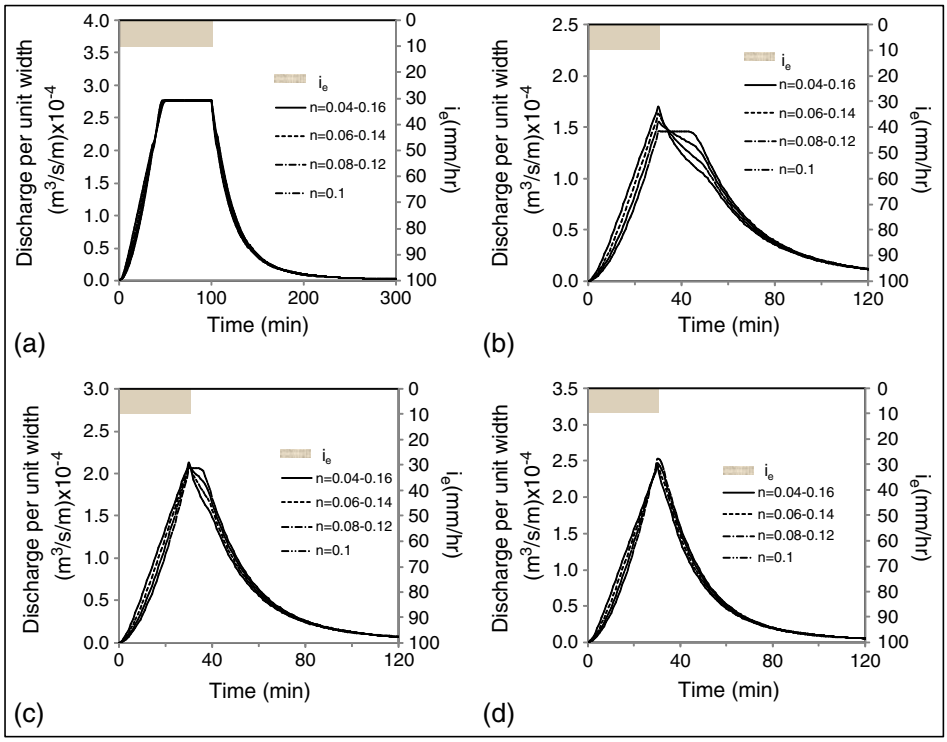

Figure 15. Hydrographs for roughness decreasing in downstream direction for different slope (rectangular plane) ((a) for slope 0.01 and td = 100 min, (b) for slope 0.01 and td = 30 min, (c) for slope 0.02 and td = 30 min and (d) for slope 0.03 and td = 30 min)

overland plane increases. Discharge with spatial roughness at simulation time of 30 min closely matches with the discharge with uniform roughness.

(c) Diverging plane

Figure 11 shows hydrographs resulting due to application of uniform rainfall of 10 mm/h for duration of 30 min on diverging plane for spatially varying roughness in range 0.04 – 0.16, 0.06 – 0.14 and 0.08 – 0.12 for different slopes of the diverging plane. Table III shows the peak discharge and time to peak discharge for td = 100 min and td = 30 min for different slopes and roughness values. As can be seen from Table III, for td = 100 min, hydrographs attained temporal equilibrium state for all roughness ranges studied, whereas for td = 30 min, hydrograph rose and receded without attaining temporal equilibrium state. For td = 30 min, the peak is 17.2%, 15.5% and 11.4% more for slopes 0.01, 0.02 and 0.03, respectively, for variable roughness between 0.04 and 0.16 than the peak discharge obtained for equivalent uniform roughness of 0.116. In diverging plane, time to peak is more than the converging plane, and the recession limb recedes slowly for similar slopes of the planes. Also the roughness variability has pronounced effect on recession limb and near the peak of rising limb. Due to divergence, the depth at the outlet is very less.

Depth, velocity and discharge profile

Figures 12, 13 and 14 show depth, velocity and discharge at distances from the upstream end along the downstream direction resulting due to application of uniform rainfall of 10 mm/h for duration of 30 min on

Table IV. Hydrograph characteristics for rectangular plane for roughness decreasing in downstream direction

Slope (m/m)	Roughness range	td = 100 min		td = 30 min	
		q_p (m^2/s/m)	t_p (min)	q_p (m^2/s/m)	t_p (min)
0.01	0.1 (uniform)	$2.778x10^{-4}$	47	$1.46x10^{-4}$	30
	0.04–0.16	$2.778x10^{-4}$	51	$1.70x10^{-4}$	30
	0.06–0.14	$2.778x10^{-4}$	51	$1.62x10^{-4}$	30
	0.08–0.12	$2.778x10^{-4}$	49	$1.55x10^{-4}$	30
0.02	0.1 (uniform)	$2.778x10^{-4}$	38	$2.06x10^{-4}$	30
	0.04–0.16	$2.778x10^{-4}$	40	$2.13x10^{-4}$	30
	0.06–0.14	$2.778x10^{-4}$	39	$2.11x10^{-4}$	30
	0.08–0.12	$2.778x10^{-4}$	38	$2.09x10^{-4}$	30
0.03	0.1 (uniform)	$2.778x10^{-4}$	33	$2.53x10^{-4}$	30
	0.04–0.16	$2.778x10^{-4}$	35	$2.42x10^{-4}$	30
	0.06–0.14	$2.778x10^{-4}$	35	$2.44x10^{-4}$	30
	0.08–0.12	$2.778x10^{-4}$	34	$2.47x10^{-4}$	30

DOI: 10.1002/hyp

diverging surface for roughness increasing downstream in the range 0.04 – 0.16 for slopes of overland planes 0.01, 0.02 and 0.03. Flow depth increases as the distance from the upstream end of overland plane increases. The computed depth of flow using spatially variable roughness is more than equivalent uniform roughness condition before simulation time of 50 min for slope of overland plane 0.01 and before simulation time of 40 min for slopes of overland plane 0.02 and 0.03.

Scenario 2: Roughness decreasing in downstream direction

(a) Rectangular plane

Figure 15 shows the resultant hydrograph obtained for spatially decreasing roughness scenario due to application of uniformly distributed rainfall at the rate of 10 mm/h for td = 100 min and td = 30 min, for slopes of overland flow planes 0.01, 0.02 and 0.03. The related information on peak and time to peak rate of runoff for different scenarios is provided in Table IV. As can be seen from Table IV, for td = 100 min, hydrographs obtained on overland flow plane slopes of 0.01, 0.02 and 0.03 attained temporal equilibrium state whereas for td = 30 min, hydrographs did not attain equilibrium state. The time to peak is more in case when roughness is decreasing in downward direction than for the scenario of increasing roughness in downward direction. For td > tc, the rising limb rose slowly as compared to roughness increasing in downstream direction due to more roughness in

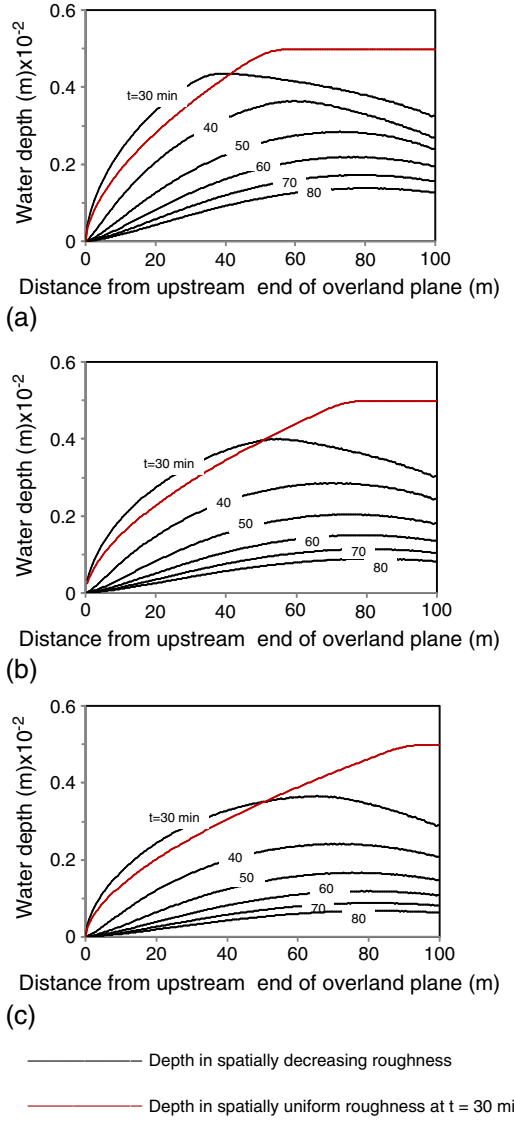

Figure 16. Water depth along the flow direction of the overland plane (rectangular plane) for decreasing roughness (0.04–0.16) at slope 0.01 (a), 0.02 (b) and 0.03 (c)), td = 30 min

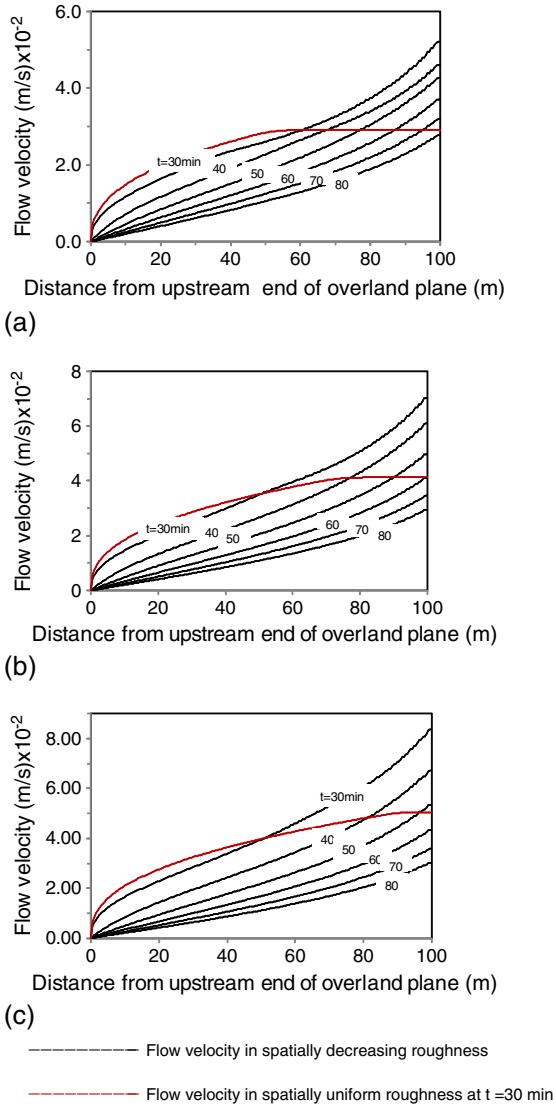

Figure 17. Flow velocity along the flow direction of the overland plane (rectangular plane) for decreasing roughness (0.04–0.16) at slope 0.01(a), 0.02 (b) and 0.03 (c), td = 30 min

DOI: 10.1002/hyp

the beginning and time to peak is more for larger range of variability of roughness. As can be seen from Table IV, for duration smaller than time of concentration, peak discharge reduces as roughness variability range reduces. Peak discharge in case of spatial roughness decreasing in downstream direction is less as compared to case of roughness increasing in downstream direction.

Depth, velocity and discharge profile

Figures 16, 17 and 18 depict depth, velocity and discharge at distance from the upstream end of plane along the downstream direction resulting due to application of uniform rainfall of 10 mm/h for the duration of 30 min on rectangular plane for the roughness range 0.04–0.16 decreasing in downstream direction and for slope of overland plane ranging from 0.01 to 0.03.For the simulation time of 30 min, the water depth starting at a distance of 40 m of overland plane from upstream end to the downstream outlet is lower than that in the spatially uniform roughness condition for all slopes. Depth increases up to certain distance and then reduces. Velocity increases along the downstream direction. Velocity increases for all time towards downstream direction whereas velocity for uniform roughness remains constant after 50 m

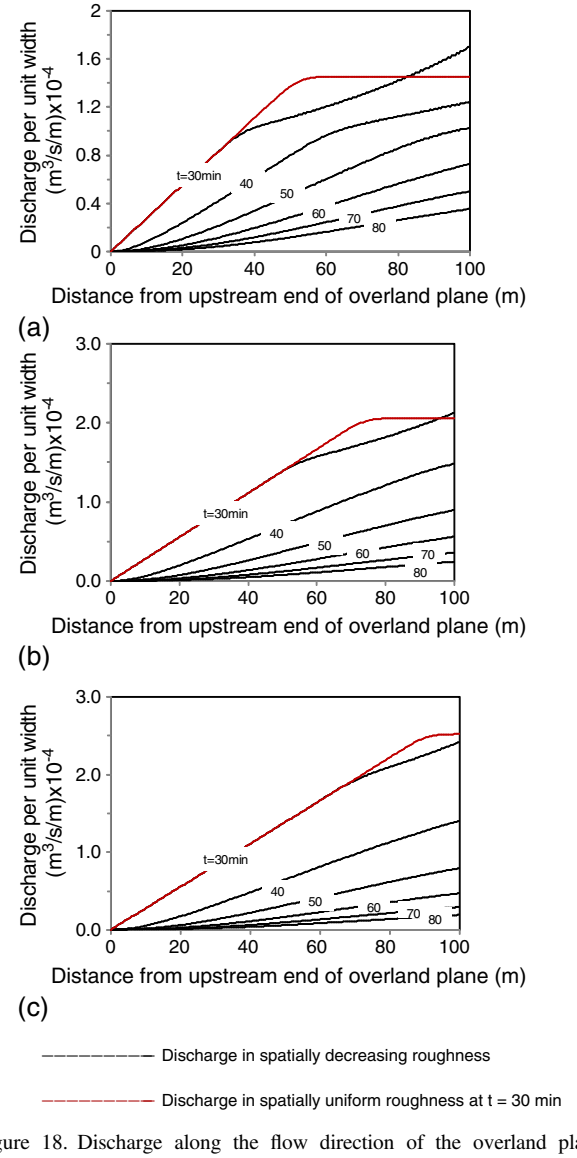

Figure 18. Discharge along the flow direction of the overland plane (rectangular plane) for decreasing roughness (0.04–0.16) at slope 0.01 (a), 0.02 (b) and 0.03 (c), td = 30 min

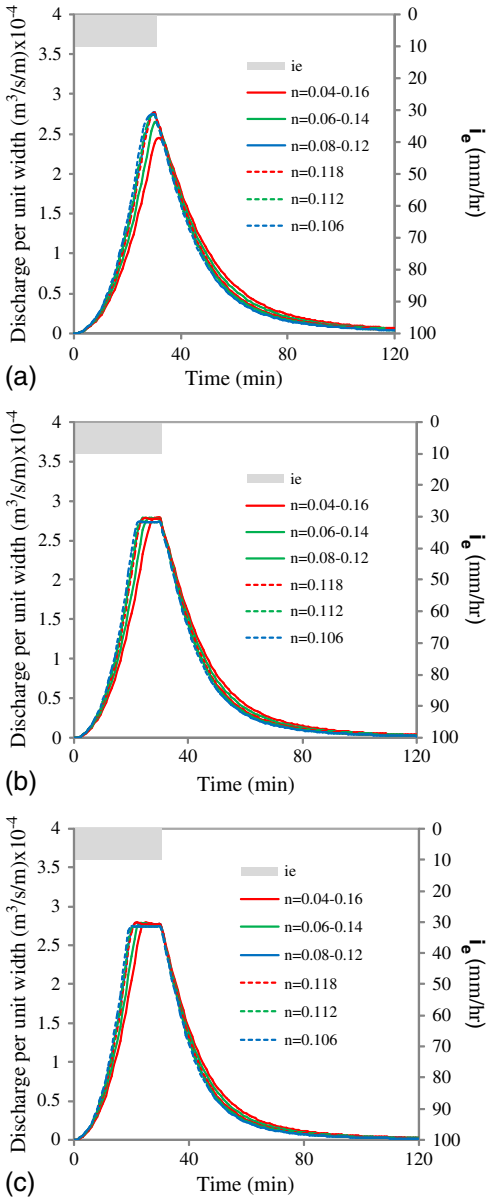

Figure 19. Hydrographs for decreasing roughness for converging plane ((a) for s = 0.01, (b) for s = 0.02 and (c) for s = 0.03), td = 30 min

DOI: 10.1002/hyp

distance from upstream end of plane. Velocity is more in decreasing roughness scenario than increasing roughness scenario. Discharge for 30 min simulation time is less than the discharge with uniform roughness for slope of plane 0.01 at 50 m, 70 m for slope of plane 0.02 and 80 m for slope of plane 0.03 from the upstream end of plane towards downstream.

(b) Converging plane

Figure 19 shows hydrographs resulting due to application of uniform rainfall of 10 mm/h for rainfall duration of 30 min on converging plane for roughness decreasing in downstream direction. Table V shows the relevant information of the hydrographs for different duration of rainfall, slope of plane and roughness value considered. The equilibrium state is attained in all roughness variability ranges and slopes for the rainfall duration of 100 min. In case of 30 min rainfall duration, equilibrium state is attained in all roughness variability ranges and slopes except for roughness in the range 0.04–0.16 and slope of 0.01. As roughness variability range increases, the time to peak increases,

Depth, velocity and discharge profile

Figures 20, 21 and 22 show depth, velocity of flow and discharge at distances from upstream end along downstream direction resulting due to application of uniform rainfall of 10 mm/h for duration of 30 min on converging plane for roughness decreasing in downstream direction. Flow depth increases as distance from upstream end along the downstream increases and the depth increases rapidly at the outlet. The computed flow depth using spatially variable roughness at simulation time 30 min is more than that obtained using equivalent uniform roughness. Computed velocity is higher when the roughness considered decreases in downstream direction than for scenario when roughness increases in downstream direction. The computed velocity of flow using uniform roughness is more than that obtained with spatially variable roughness at simulation time of 30 min. Discharge increases rapidly as distance increases in downstream direction.

Table V. Hydrograph characteristics for converging plane for roughness decreasing in downstream direction

Slope (m/m)	Roughness range	td = 100 min		td = 30 min	
		q_p (m^2/s/m)	t_p (min)	q_p (m^2/s/m)	t_p (min)
0.01	0.04–0.16	2.778×10^{-4}	33	2.660×10^{-4}	32
	0.118 (uniform)	2.778×10^{-4}	32	2.745×10^{-4}	30
	0.06–0.14	2.778×10^{-4}	30	2.778×10^{-4}	30
	0.112 (uniform)	2.778×10^{-4}	31	2.775×10^{-4}	31
	0.08–0.12	2.778×10^{-4}	27	2.778×10^{-4}	30
	0.106 (uniform)	2.778×10^{-4}	30	2.778×10^{-4}	30
0.02	0.04–0.16	2.778×10^{-4}	23	2.778×10^{-4}	23
	0.118 (uniform)	2.778×10^{-4}	25	2.778×10^{-4}	25
	0.06–0.14	2.778×10^{-4}	23	2.778×10^{-4}	23
	0.112 (uniform)	2.778×10^{-4}	24	2.778×10^{-4}	24
	0.08–0.12	2.778×10^{-4}	22	2.778×10^{-4}	22
	0.106 (uniform)	2.778×10^{-4}	23	2.778×10^{-4}	23
0.03	0.04–0.16	2.778×10^{-4}	23	2.778×10^{-4}	23
	0.118 (uniform)	2.778×10^{-4}	22	2.778×10^{-4}	22
	0.06–0.14	2.778×10^{-4}	22	2.778×10^{-4}	22
	0.112 (uniform)	2.778×10^{-4}	21	2.778×10^{-4}	21
	0.08–0.12	2.778×10^{-4}	21	2.778×10^{-4}	21
	0.106 (uniform)	2.778×10^{-4}	20	2.778×10^{-4}	20

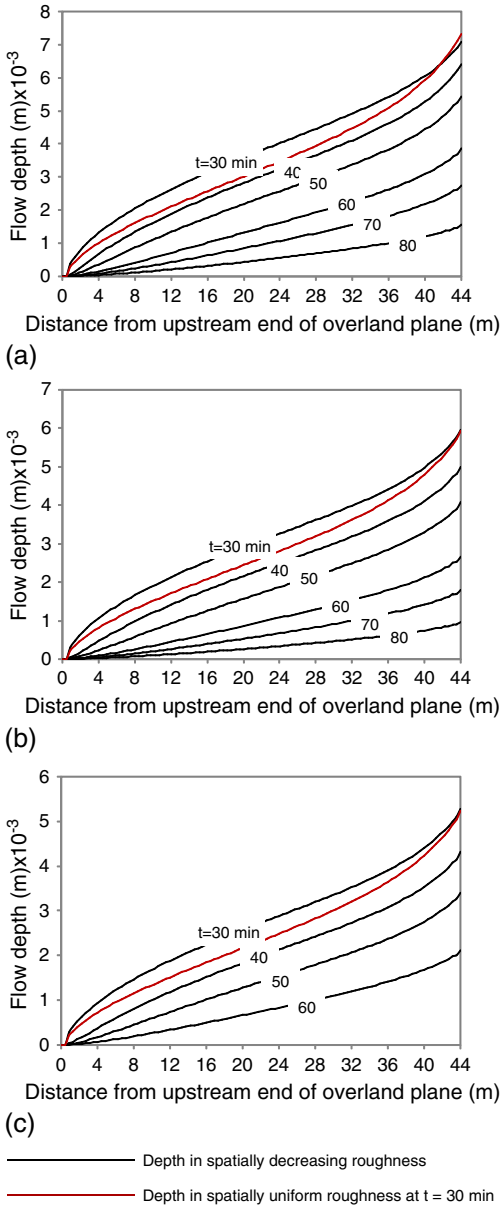

Figure 20. Water depth along the flow direction of the converging plane for decreasing roughness (0.04–0.16) at slope 0.01(a), 0.02 (b) and 0.03 (c)), td = 30 min

DOI: 10.1002/hyp

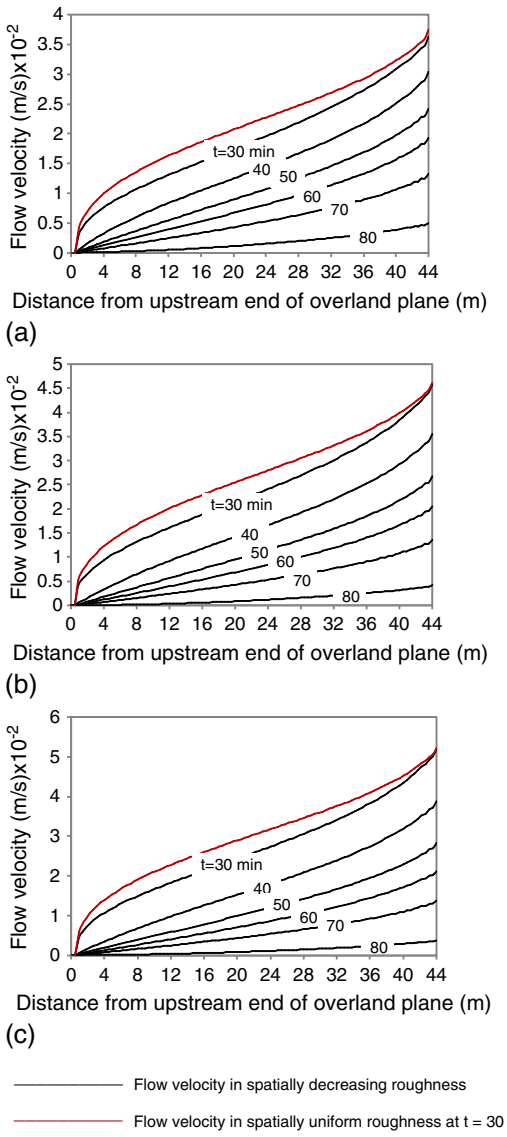

Figure 21. Flow velocity along the flow direction of the converging plane for decreasing roughness (0.04–0.16) at slope 0.01(a), 0.02 (b) and 0.03 (c), td = 30 min

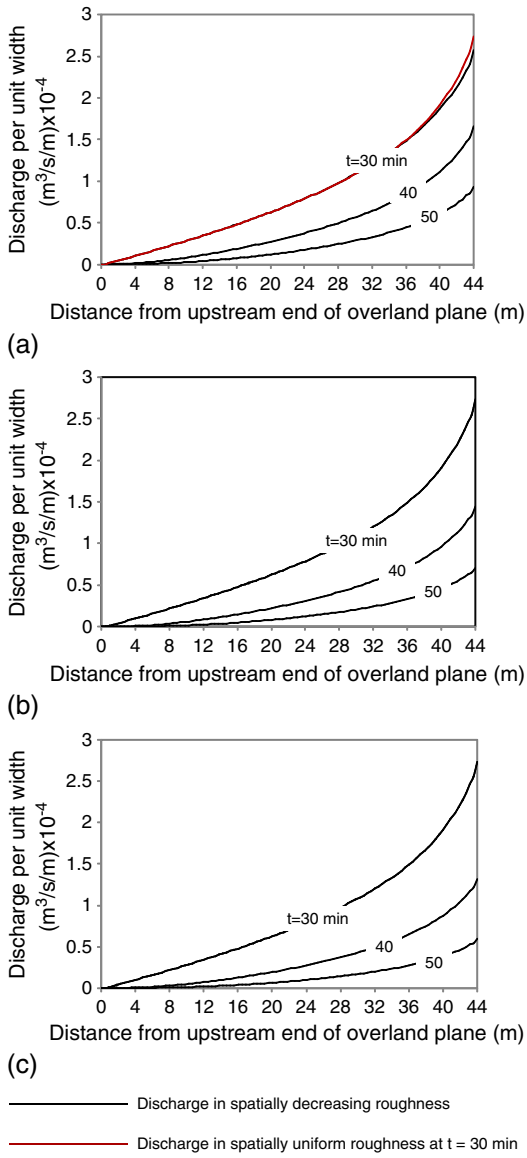

Figure 22. Discharge along the flow direction of the converging plane for decreasing roughness (0.04–0.16) at slope 0.01(a), 0.02 (b) and 0.03 (c), td = 30 min

(c) Diverging plane

Figure 23 shows hydrographs resulting due to application of rainfall at 10 mm/h for different ranges of roughness and slope of 0.01, 0.02 and 0.03 for diverging plane for roughness decreasing in downstream direction. Table VI shows the relevant information of the hydrograph. For td =100 min, computed hydrograph attained equilibrium state for all overland plane slopes and variability of roughness. However, for td = 30 min, computed hydrograph could not attain equilibrium state. The roughness has effect on flow hydrograph between the peak and the end of the recession limb.

Depth, velocity and discharge profile

Figures 24, 25 and 26 depict depth, velocity and discharge at distance from upstream end along the downstream direction resulting due to application of uniformly distributed rainfall at a rate of 10 mm/h on diverging plane for roughness decreasing in downstream direction. Depth of flow increases as distance downstream increases and then remains constant for simulation time 30, 40, 50 and 60 min. Velocity increases as the distance along the downstream increases. Velocity attained by uniform roughness is more than that of roughness spatially variable. The discharge attained with uniform roughness closely matches with the

DOI: 10.1002/hyp

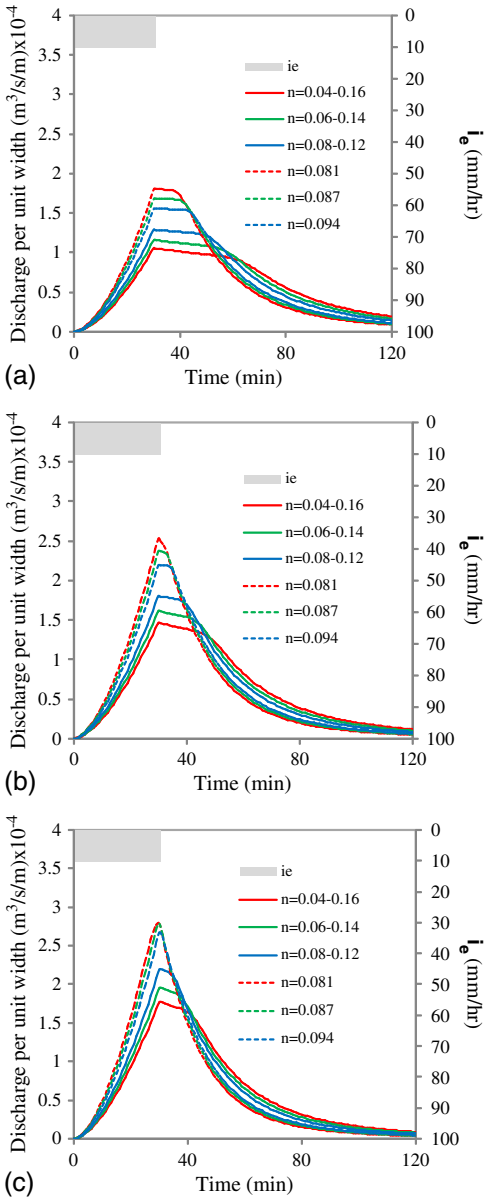

Figure 23. Hydrographs for decreasing roughness for diverging plane ((a) for s = 0.01, (b) for s = 0.02 and (c) for s = 0.03) td = 30 min, td = 30 min

discharge with spatial roughness up to certain distance and then becomes more than that.

Scenario 3: Roughness distributed randomly

For this scenario, the roughness values in the range 0.04 to 0.16 generated randomly using EXCEL package are used to generate runoff hydrograph using rainfall of intensity 10 mm/h for 30 min duration with slope of domain as 0.01. The values of random roughness in these three sets vary between 0.04 and 0.16, but the internal sequencing of value of Manning's roughness is varying randomly, and hence

Table VI. Hydrograph characteristics for diverging plane for roughness decreasing in downstream direction

Slope	Roughness range	td = 100 min		td = 30 min	
		q_p (m^2/s/m)	t_p (min)	q_p (m^2/s/m)	t_p (min)
0.01	0.04–0.16	2.778×10^{-4}	62	1.05×10^{-4}	30
	0.081 (uniform)	2.778×10^{-4}	41	1.801×10^{-4}	30
	0.06–0.14	2.778×10^{-4}	57	1.16×10^{-4}	30
	0.087 (uniform)	2.778×10^{-4}	43	1.677×10^{-4}	30
	0.08–0.12	2.778×10^{-4}	53	1.29×10^{-4}	30
	0.094 (uniform)	2.778×10^{-4}	45	1.552×10^{-4}	30
0.02	0.04–0.16	2.778×10^{-4}	49	1.46×10^{-4}	30
	0.081 (uniform)	2.778×10^{-4}	33	2.533×10^{-4}	30
	0.06–0.14	2.778×10^{-4}	45	1.62×10^{-4}	30
	0.087 (uniform)	2.778×10^{-4}	34	2.372×10^{-4}	30
	0.08–0.12	2.778×10^{-4}	42	1.81×10^{-4}	30
	0.094 (uniform)	2.778×10^{-4}	36	2.195×10^{-4}	30
0.03	0.04–0.16	2.778×10^{-4}	43	1.77×10^{-4}	30
	0.081 (uniform)	2.778×10^{-4}	29	2.778×10^{-4}	30
	0.06–0.14	2.778×10^{-4}	40	1.96×10^{-4}	30
	0.087 (uniform)	2.778×10^{-4}	30	2.778×10^{-4}	30
	0.08–0.12	2.778×10^{-4}	37	2.20×10^{-4}	30
	0.094 (uniform)	2.778×10^{-4}	32	2.670×10^{-4}	30

these three sets produced different output hydrographs. Figures 27, 28 and 29 show the hydrographs produced by three sets of randomly distributed roughness for rectangular, converging and diverging planes respectively. These hydrographs demonstrate that different set of random values results in different time to peak and shape of hydrograph for rectangular and diverging plane. In case of converging plane, the shape of computed hydrographs remains almost similar for different sets of random roughness values indicating stronger influence of converging geometry than effect due to variation of roughness sequence on computed runoff hydrograph.

DISCUSSION

Results presented in earlier sections reveal that whatever the geometry of the plane, the peak runoff occurs earlier in scenario 1 (roughness increasing downstream) than in scenario 2 (roughness decreasing downstream). This could be attributed to the fact that in the Darcy–Weisbach relationship, S_f is approximated as

$$S_f = \frac{fu^2}{8gh} \tag{29}$$

where f is the Darcy–Weisbach's friction factor. Equating this equation with Manning–Stickler's friction law

DOI: 10.1002/hyp

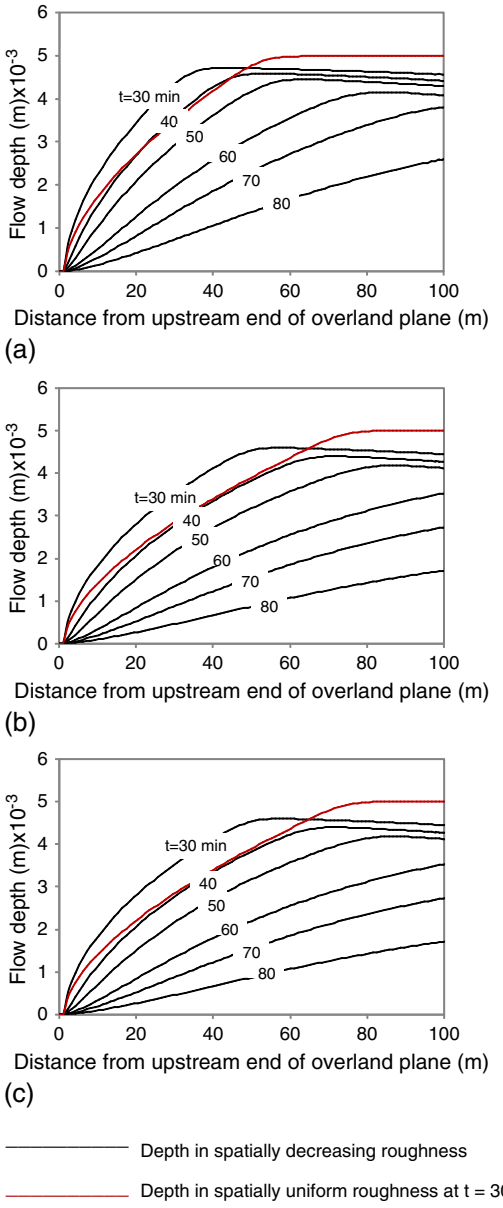

Figure 24. Water depth along the flow direction of the diverging plane for decreasing roughness (0.04–0.16) at slope 0.01(a), 0.02 (b) and 0.03 (c)), td = 30 min

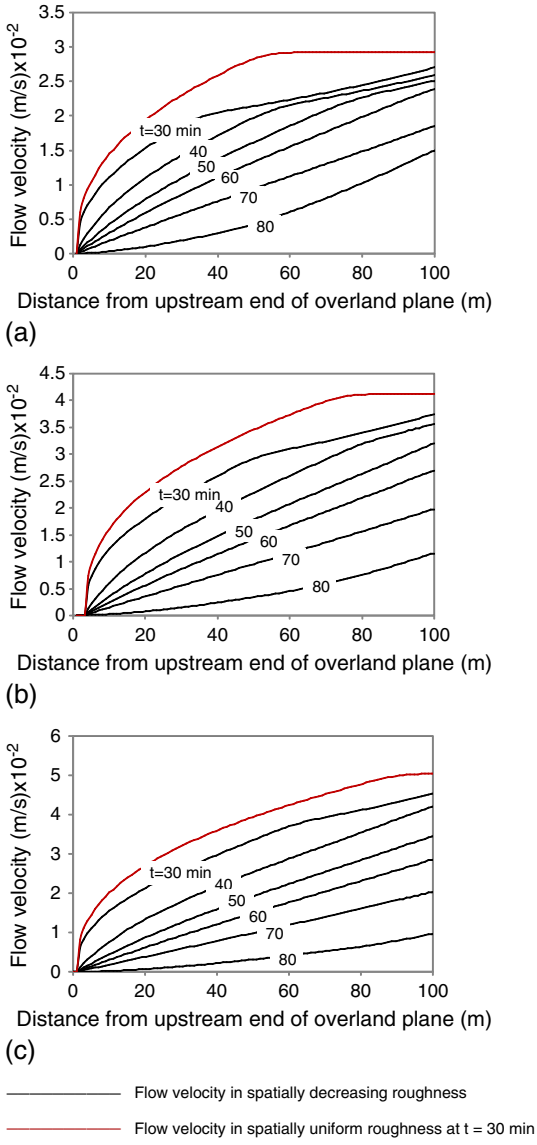

Figure 25. Flow velocity along the flow direction of the diverging plane for decreasing roughness (0.04–0.16) at slope 0.01(a), 0.02 (b) and 0.03 (c), td = 30 min

(Equation (7)), Darcy–Weisbach relationship with a friction factor f(h) becomes

$$f(h) = \frac{8gn^2}{h^{\frac{1}{3}}} \tag{30}$$

Where, $f(h)$ is a friction factor as a function of flow depth h, g is acceleration due to gravity and n is Manning's roughness coefficient. Equation (30) clearly indicates that the friction factor decreases with the water depth h. Hence, for the roughness scenario 1, at the top of the domain where water depth is more due to less value of Manning's roughness, the friction factor is very low, and flow velocity is more. Also, as distance towards downstream increases, the depth increases, so effect of increased roughness is reduced due to more depth of water. Friction factor also remains low. Therefore, peak arrives faster. Whereas in scenario 2, at the top of the domain where water depth is very thin, the friction factor is very high and flow velocity is very small. This behavior is enhanced when roughness decreases from top to the bottom of the domain, but the depth attained along the distance is less than the scenario 1, therefore, comparatively lower velocities than the scenario 1. Also, according to Manning's equation, velocity is inversely proportional to roughness and directly proportional to square root of slope. Observing hydrographs of rectangular, converging and diverging sections

DOI: 10.1002/hyp

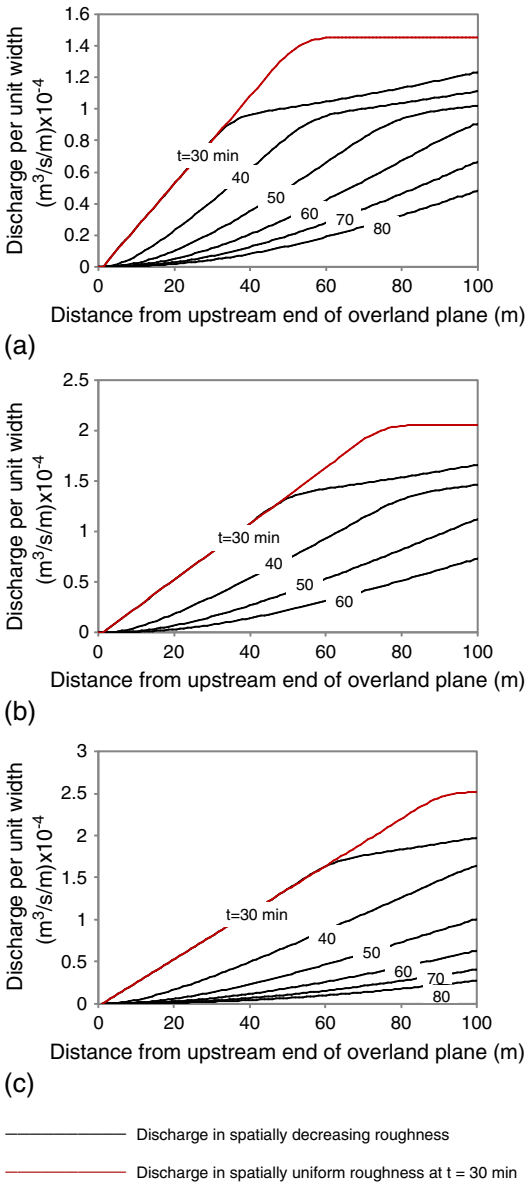

Figure 26. Discharge along the flow direction of the diverging plane for decreasing roughness (0.04–0.16) at slope 0.01(a), 0.02 (b) and 0.03 (c), td = 30 min

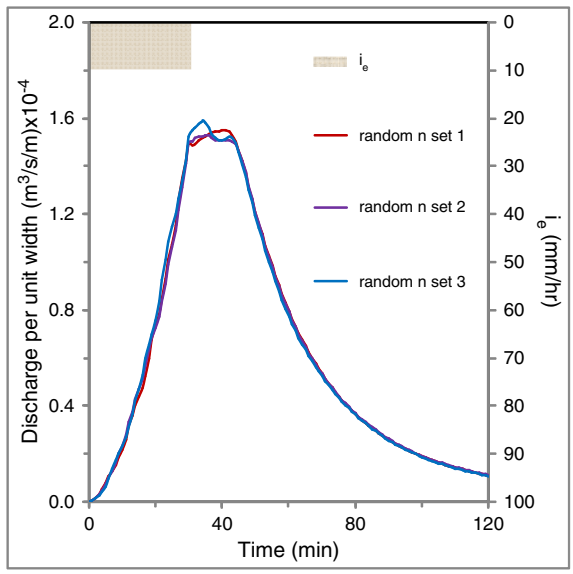

Figure 27. Hydrograph for roughness distributed randomly for different set of random roughness (rectangular plane), td = 30 min

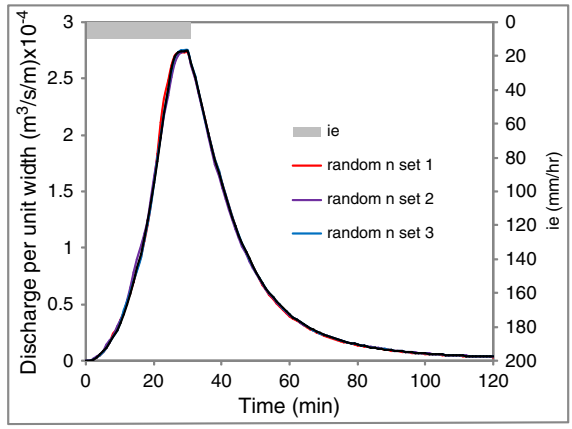

Figure 28. Hydrograph for roughness distributed randomly for different set of random roughness (converging plane), td = 30 min

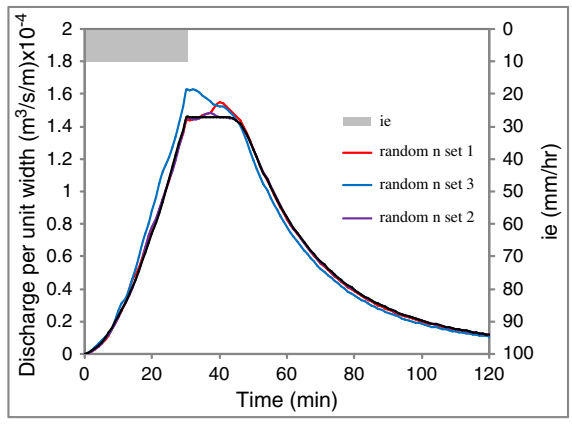

Figure 29. Hydrograph for roughness distributed randomly for different set of random roughness (diverging plane), td = 30 min

(Figures 3, 7, 11, 15, 19 and 23), it is found that hierarchically, the influence of geometry on overland flow is stronger than the influence of slope and that the influence of slope is stronger than the influence of roughness.

In practical situations, we may imagine roughness increasing in downstream direction (scenario 1) as an overland flow plane where fallow land is at the top of the domain with a decreasing eroded surface (or increase in vegetation) from top to the bottom. On the other hand, scenario 2 could be visualized as a hill slope where dense vegetation is found at top of the hill, and cultivated land followed by fellow land is at the end of the hill slope. Then, the peak of the runoff hydrograph occurs earlier for

DOI: 10.1002/hyp

scenario 1 as compared to scenario 2 due to very low friction factor and more velocity at the top of the domain in scenario 1. It implies that the time to peak can be delayed by progressively increasing the roughness, i.e. vegetating the surface with grass or cultivating close growing agricultural crops in downstream flow direction. It could also be helpful in limiting the overland flow and moderation of flood events.

CONCLUSION

The effect of spatial variation of roughness on overland flow hydrograph is studied using numerical simulations for rectangular, converging and diverging planes for different slopes of the planes using two rainfall durations of constant intensity to understand the overland flow characteristics with equilibrium and non-equilibrium discharge cases. Three scenarios of spatially variable Manning's roughness viz. roughness increasing in downstream direction, roughness decreasing in downstream direction and roughness distributed at random are considered. The range of Manning's roughness for these scenarios is chosen because between 0.04 and 0.16 in natural watersheds, the variability of Manning's roughness for different landuse classes is generally professed within these ranges. Results of the study indicate that variability of Manning's roughness has significant effect on overland flow in terms of depth, velocity of flow along the distance from upstream to downstream and overall shape of the overland flow hydrograph for different geometric surfaces and spatial patterns of Manning's roughness distribution. The converging plane attains equilibrium state early as compared to rectangular and diverging plane. Different set of random values of roughness results in different time to peaks and shapes of hydrograph for rectangular and diverging planes. However, in case of converging plane, the shape of computed hydrographs remains almost similar for different sets of random roughness values indicating stronger influence of converging geometry than effect due to variation of roughness sequence on computed runoff hydrograph. The spatial roughness has more effect on diverging section followed by rectangular plane and converging plane. Hierarchically, the influence of geometry on the overland flow is stronger than the influence of slope, and that the influence of slope is stronger than the influence of roughness. In practical situations, we may imagine roughness increasing in downstream direction (scenario 1) as an overland flow plane where fallow land is at the top of the domain with a decreasing eroded surface (or increase in vegetation) from top to the bottom. On the other hand, scenario 2 could be visualized as a hill slope where dense vegetation is found at top of the hill and cultivated land followed by fellow land is at the end of the hill slope. Then, the peak of the runoff hydrograph occurs earlier for scenario 1 as compared to scenario 2 due to very low friction factor and more velocity at the top of the domain in scenario 1. It implies that the time to peak can be delayed by progressively increasing the roughness, i.e. vegetating the surface with rigid grass or cultivating close growing agricultural crops in downstream flow direction. The results obtained from this study could be helpful in devising moderation strategies for regulating overland flow and flood events.

ACKNOWLEDGEMENTS

The authors wish to sincerely thank anonymous reviewers whose comments greatly improved the quality of this paper.

LIST OF NOTATIONS

h	depth of flow
q	discharge per unit width
i_e	rainfall excess
S	slope of the surface
W	width of rectangular plane
L	length of rectangular plane
R_0	length of converging section
c	degree of convergence
Θ	interior angle
R	length of diverging section
a	degree of divergence
S_0	bed slope
S_f	friction slope
n	Manning's roughness coefficient
u	velocity of flow
x	distance along the flow direction in case of rectangular plane
r	distance along the flow direction in case of converging and diverging plane
t	time
td	duration of rainfall
t_p	time to peak
t_c	time of concentration
f	friction factor
Δt	time interval for flow routing
Δx	space interval for flow routing
i	space node
k	time node
N	total number of space nodes
$*$	represents values of variables at the end of predictor step
$**$	represents values of variables at the end of corrector step
g	acceleration due to gravity

DOI: 10.1002/hyp

REFERENCES

Agiralioglu N, Singh VP. 1980. 1. A mathematical investigation of diverging overland flow, 2. Numerical solutions and applications. Tech. Rep. MSSU-EIRS-CE-80-4, Engngand Industrial Res. Station, Mississippi State University, Mississippi State, Mississippi.

Beven K. 1978. The hydrological response of head water and side slope areas. *Hydrological Sciences Bulletin* **23**(4): 419–437.

Campbell SY, Parlange JY, Rose CW. 1984. Overland flow on converging and diverging surface – kinematic model and similarity solutions. *Journal of Hydrology* **67**: 367–374.

Chaudhry MH. 1993. Open Channel Flow. Prentice Hall: Eaglewood Cliffs, NJ.

Chow VT. 1959. Open Channel Flow. McGraw-Hill: New York.

Dammuller D, Bhallamudi SM, Chaudhry MH. 1989. Modeling of unsteady flow in curved channels. *Journal Hydraulic Engineering, American Society of Civil Engineers* **115**(11): 1479–1495.

Engman ET. 1986. Roughness coefficients for routing surface runoff. *Journal of Irrigation and Drainage Engineering* **112**(1): 39–53.

Fennema RJ, Chaudhry HM. 1986. Explicit numerical schemes for unsteady free-surface flows with shocks. *Water Resources Research* **22**(13): 1923–1930.

Fennema RJ, Chaudhry HM. 1987. Simulation of one-dimensional dam-break flows. *Jour. hydraulic Research*, Inter. Assoc. for Hydraulic Research **25**(1): 41–51.

Gonwa WS, Kavvas ML. 1986. A modified diffusion equation for flood propogation in trapezoidal channel. *Journal of Hydrology* **83**: 119–136.

Govindaraju RS, Kavvas ML, Jones SE. 1990. Approximate analytical solution for overland flows. *Water Resources Research* **26**(12): 2903–2912.

Hairsine SY, Parlange JY. 1986. Kinematic shock waves on curved surfaces and application to the cascade approximation. *Journal of Hydrology* **87**: 187–200.

Henderson FM, Wooding RA. 1964. Overland flow and groundwater from a steady rainfall of finite duration. *Journal of Geophysical Research* **69**(8): 1531–40.

Huang J-K, Lee KT. 2009.Influences of spatially heterogeneous roughness on flow hydrographs. *Advances in water resources* **32**: 1580–1587.

Jain MK, Singh VP. 2005. DEM based modeling of surface runoff using diffusion wave equation. *Journal of Hydrology* **302**(1-4): 107–126.

Jain MK, Kothyari UC, RangaRaju KG. 2004. GIS based distributed rainfall – runoff model. *Journal of Hydrology* **299**(1-2): 107–135.

Langford KJ, Turner AK. 1973. An experimental study of the application of kinematic wave theory to overland flow. *Journal of Hydrology* **18**: 125–145.

Lehrsch GA, Whisler FD, Romkens MJM. 1987. Soil surface roughness as influenced by selected soil physical properties. *Soil and Tillage research* **10**: 197–212.

Lehrsch GA, Whisler FD, Romkens MJM. 1988. Spatial variation of parameters describing soil surface roughness. *Soil Science Society of America Journal* **52**(2): 311–319.

MacCormack RW. 1969. The effect of viscosity in hypervelocity impact cratering. Amer. Inst. Aero.Astro., Paper 69-354, Cincinnati, OH.

Melek K-A, Medina MA. 2007. Kinematic and diffusion waves: Analytical and numerical solutions to overland and channel flow. *Journal of Hydraulic Engineering* **133**(2): 217–228.

Moore ID. 1985. Kinematic overland flow: Generalization of Rose's approximate solution. *Journal of Hydrology* **82**: 233–245.

Morris EM. 1979. The effect of the small-slope approximation and lower boundary conditions on solutions of the Saint-Venant equations. *Journal of Hydrology* **40**: 31–47.

Nejafi MS. 2003. Watershed modeling of rainfall excess transformation into runoff. *Journal of Hydrology* **270**: 273–281.

Ponce VM. 1989. Engineering Hydrology: Principles and Practices. Prentice Hall: Eaglewood Cliffs, New Jersey, USA.

Shen HW, Julien PY. 1992. Erosion and Sediment Transport. Chap. 12. In Handbook of Hydrology, Maidment DR (ed). McGraw Hill: New York; 12.1–12.61.

Singh VP. 1996. Kinematic wave modeling in water resources. John Wiley and sons Inc: NY; 1399.

Singh VP, Aravamuthan V. 1997.Accuraccy of kinematic wave and diffusion wave approximations for time-independent flows with momentum exchange included. *Hydrological Processes* **11**: 511–532.

Singh VP, Aravamuthan V. 1998.Accuraccy of kinematic wave and diffusion wave approximations for time-independent flows with infiltration included. *Hydrological Processes* **12**: 1951–1961.

Singh VP, Frevert D. 2002. Mathematical models of small watershed hydrology and applications. Water Resources Publication: Highlands Ranch, Colorado, USA.

Singh VP, Woolhiser DA. 1976. A nonlinear kinematic wave model for watershed surface runoff. *Journal of Hydrology* **31**: 221–243.

Singh VP, Woolhiser DA. 2002. Mathematical modeling of watershed hydrology. *Journal of Hydrologic Engineering* **7**(4): 270–292.

Tayfur G, Kavvas ML, Govindaraju RS, Storm DE. 1993. Applicability of St Venantequations for two-dimensional overland flow over rough infiltrating surfaces. *J. Hydraulic Eng.*, ASCE, **119**(1): 51–63.

Tsai TL, Yang JC. 2005.Kinematic wave modeling of overland flow using characteristic method with cubic spline interpolation. *Advances in Water Resources* **28**(7): 661–670.

Vieux BE, Farajalla NS. 1994.Capturing the essential spatial variability in distributed hydrologic modeling: hydraulic roughness coefficient. *International Journal of Hydrologic Processes* **8**: 221–236.

Wang M, Hjelmfelt AT. 1998. DEM based overland flow routing model. *J. Hydrologic Eng.*, ASCE, **3**(1): 1–8.

Wong TSW. 1997. Discussion of 'search for physically based runoff model – a hydrologic el dorado?' by D. A. Woolhiser. *Journal of Hydraulic Engineering*, ASCE, **123**(9): 830.

Woolhiser DA. 1969. Overland flow on a converging surface. *Trans. A.S. A.E.* **12**(4): 460–462.

Wu YH, Yevjevich V, Woolhiser DA. 1978. Effects of surface roughness and its spatial distribution on runoff hydrographs, hydrol. Pap.96, Colo. State Univ., Fort Collins.

Wu YH, Woolhiser DA, Yevjevich V. 1982.Effects of spatial variability of hydraulic resistance of runoff hydrographs. *Journal of Hydrology* **9**: 231–248.

Yu US, McNown JS. 1964.Runoff from impervious surface. *Journal of Hydraulic Research* **1**: 3–24.

DOI: 10.1002/hyp